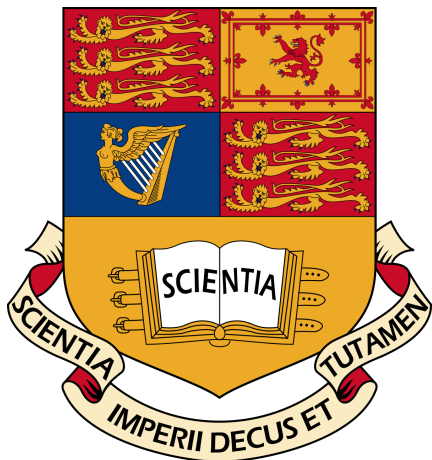


Imperial College London

Department of Electrical and Electronic Engineering

Final Year Project Report 2018



Project Title: **Optimizing the operation of battery storage with the consideration of life-time degradation**

Student: **Theo C. Franquet**

CID: **00967383**

Course: **EEE**

Project Supervisor: **Dr Fei Teng**

Second Marker: **Dr Bikash Pal**

Abstract

Rechargeable battery energy storage technologies are competitive candidates in the electricity markets, mostly thanks to their ability to charge and discharge with high efficiency and at high rates. As the price of batteries faces decline on a yearly basis, profitability of owning and operating battery assets is increasing. This project delves into a crucial limiting factor of battery technology proliferation in grid support applications: battery aging. Battery energy storage in general is characterized by limited lifetime, in the order of a few years, which is very dependent on cycling behavior. This paper explores and evaluates various ways of accurately modeling the aging cost of battery storage, in irregular cycling conditions more specifically. Semi-empirical degradation models are selected to form chemistry specific aging cost models. Individual degradation models are based on existing research for power system applications, and backed by fundamental electrochemical theory and experimental evidence. Multiple models are presented in accordance with the specific battery technology at use. In our case, models are evaluated for both Li-Ion and Vanadium Redox Flow batteries. The aging cost model uses a cycle-counting method to evaluate the daily loss of cycle life for a specific battery operation scheme. It also incorporates a state-of-charge stress model. The usefulness of this degradation cost model is then illustrated through a battery capacity bidding optimization problem on day-ahead electricity markets, taking aging into consideration. Results illustrate the impact and benefits of taking battery degradation costs into account on the optimal bidding strategy for different battery storage technologies.

Acknowledgments

First and foremost I would like to acknowledge my project supervisor Dr. Fei Teng for granting me the opportunity to work on this captivating and challenging project. I am thankful for his continuous support and insightful advice throughout the year.

I would like to express my deep and sincere gratitude to all my friends for continuously providing positive vibes in the good as much as in the hard times. A special thank you to the Remyboyz and members of the Nevern Corporation for being a part of this unforgettable journey at Imperial College.

Finally, but by no means last, a special mention goes to Eric Estornel, Nicolas Jaar and David August for their respective memorable Boiler Room DJ sets which have helped me achieve high levels of productivity on numerous occasions during the course of this project.

Contents

1	Introduction	8
1.1	The Electrical Grid	8
1.2	Optimal Battery Management	9
1.3	Cost of Battery Storage Degradation	10
1.4	Motivation & Report Structure	10
2	Background	12
2.1	Creating Value with Battery Storage	12
2.1.1	Overview	12
2.1.2	Service Comparison	16
2.2	Literature Review	17
2.2.1	Optimal Battery Control Considering Battery Aging	17
2.2.2	Comparative Study of Battery Storage Technologies	19
3	Aging Cost Model Analysis & Design	24
3.1	Battery Storage Degradation Modeling	24
3.1.1	Introduction to Aging Mechanisms and Modeling	24
3.1.2	DOD Stress Model	27
3.1.3	SOC Stress Model	32
3.1.4	Calendar Life	34
3.2	Lifetime Maximization vs. Aging Cost Minimization	35
4	Optimal Bidding Strategy Model Considering Cycle Aging Costs	38
4.1	Markets Operation and Specificities	38
4.2	Formulation of the Optimisation Problem	41
4.3	Implementation	50
4.4	Testing and Analysis	53
5	Conclusion & Future Work	65

Nomenclature

β_t	Average energy consumed in regulation within hour t for 1MW committed regulation capacity	day	Superscript for daily variables
\mathbf{d}^{half}	Vector of SOC half cycles	E_t	Battery's energy stored at time t , MWh
\mathbf{x}	Vector of discrete SOC values	E_{max}	Energy capacity of battery unit, MWh
ΔE_t	Battery's energy level change at time t , MWh	Eff	Battery energy efficiency
γ^{res}	Probability of reserve deployment	H	Set of time
ρ	SOC stress multiplier	K	Set of intra-hour half cycles
σ	SOC level, %	kp	DOD stress model empirical coefficient
C	Set of hour to hour half cycles	ks	SOC stress model empirical coefficient
c_m	Daily cost of maintenance, \$/MW	$Loss_{cycle}$	Loss of cycle life, %
C_{batt}	Cost of battery storage unit. \$	n_d	Number of cycles at a DOD of d
$Cap_t^{(.)}$	Capacity bid in market at time t , MW	n_{100}^{eq}	Equivalent number of 100% DOD cycles
$Cost_{cycle}$	Cost of cycle aging, \$	N_d^{fail}	Maximum number of charge discharge cycles at DOD of d before battery failure
d	Depth of Discharge (DOD)	$P_t^{(.)}$	Market price at time t , \$/MW
		P_{life}	Lifetime maximization problem
		P_{max}	Power capacity of battery unit, MW
		P_{profit}	Aging cost minimization problem
		ref	Subscript for reference values
		$Score^{perf}$	Regulation performance score
		T_{cycle}	Cycle lifetime, days
		T_{float}	Calendar lifetime, days

List of Figures

2.1	Overview of System Sell and System Buy Prices mechanisms	13
2.2	Typical summer and winter demands	14
2.3	Simplified illustration of peak-shaving mechanism	14
2.4	Annual state of charge (SOC) profile of battery storage participating in frequency regulation (left) and the corresponding histogram of the number of cycles in function of DOD (right)	18
2.5	High-level diagram of Li-Ion battery operation. [21]	19
2.6	High level VRB functional diagram	21
2.7	Accumulated cycle costs of various ES Technologies	22
3.1	Li-Ion molecular level degradation mechanisms, their causes, effects and relations to degradation modes	25
3.2	Basic configuration of a Thevenin-based electrical battery model [49]	26
3.3	An example of Li-Ion degradation curve	28
3.4	Cycle life vs. DOD for different values of k_p	29
3.5	Cycle life vs. DOD for different forms of $f(d)$	29
3.6	Example of rainflow counting algorithm output	31
3.7	Capacity loss of Li-Ion battery for various operating SOC ranges	33
4.1	Example dispatch for multiple service provision	39
4.2	1h EFR Signal and corresponding battery SOC profile	40
4.3	Typical day-ahead electricity prices in US dollar	41
4.4	High level structure of optimal bidding strategy model	51
4.5	Components of the objective function	52
4.6	Optimal bidding strategies and energy curves of VRB storage. (top) Without consideration of degradation costs, (bottom) with consideration of degradation costs	55
4.7	Optimal bidding strategies and energy curves of Li-Ion storage. (top) Without consideration of degradation costs, (bottom) with consideration of degradation costs	57

4.8	Optimal bidding strategies and energy curves of storage when participating to energy arbitrage only. (top) VRB technology (bottom) LFP technology	59
4.9	Optimal bidding strategies and energy curves of storage when participating to reserves and energy markets. (top) VRB technology (bottom) LFP technology	60
4.10	Optimal bidding strategies and energy curves of storage when participating to regulation and energy market. (top left) VRB technology without aging cost consideration (top right) VRB technology with aging cost consideration (bottom left) LFP technology without aging cost consideration (bottom right) LFP technology with aging cost consideration	62
4.11	Optimal bidding strategies and energy curve of LTO battery storage when participating to reserves, regulation and energy markets without aging costs consideration . . .	63
4.12	Optimal bidding strategies and energy curve of LTO battery storage when participating to reserves, regulation and energy markets with aging costs consideration (top) $ks = 0.8$, (middle) $ks = 1$, (bottom) $ks = 1.2$	64

List of Tables

2.1	Value generation methods for battery storage	16
2.2	Summary comparison of cost and aging characteristics of LFP, LTO and VRB batteries	23
3.1	Summary of strengths and challenges of degradation models	27
4.1	Daily revenues, costs and aging data for VRB participating in energy, reserves and regulation markets	56
4.2	Daily revenues, costs and aging data for LFP participating in energy, reserves and regulation markets	56
4.3	Daily revenues, costs and aging data for VRB and LFP participating in energy and reserve markets	61
4.4	Daily revenues, costs and aging data for VRB and LFP participating in energy and regulation markets	61

Chapter 1

Introduction

1.1 The Electrical Grid

Historically, electricity has differentiated itself from other conventional commodities by the fact that its consumption should be matched by supply in real time, and that significantly large amounts of energy could not be stored economically. This constraint has made way to numerous crucial challenges to be addressed by entities connected to the electrical grid. The impossibility to store electricity, coupled with large load swings and inexact load forecasting is exerting great amounts of stress on the grid, even today, causing risks of:

- Blackouts due to upstream plant outage
- Large frequency deviations leading to physical damage of connected equipment
- Inefficient supply and high generation costs
- Extremely volatile electricity market prices

Concerns regarding climate change and greenhouse gas emissions by conventional power plants more specifically, have encouraged the penetration of MW and kW scale renewable generation within the global energy mix. This momentum is set to persist, supported by governmental ambitions to massively increase electricity generation from renewable sources of energy. Rapid expansion of wind

and photo voltaic (PV) generation penetration is characterized by inflexibility of power output which is strongly dependent on changing environmental conditions. This transformation is also creating new challenges at the generation, transmission and at the distribution levels such as:

- Load balancing
- Large frequency and voltage deviations
- Duck curve effect for PV dominant locations

Significant research and development into large scale energy storage (ES) technologies has been made in recent years, in an attempt to respond to the challenges mentioned above. Battery based ES has proven potential to support grid reliability and stability as well as generating revenues on the electricity markets. Battery storage owners face the need to have a viable business case to capture new and diverse revenue streams to justify significant financial investments made in batteries. The electricity market has been evolving accordingly to accommodate ES infrastructure owners. Consequently, notable research efforts have been made to assess and encourage technological and economic viability of said infrastructure, responding to the increasing demand for renewable energy integration and growing willingness to strengthen the grid. A sharp decrease in battery capacity costs, coupled with the creation of suited market structures have together made it possible to generate significant amounts of profit for battery storage owners in certain scenarios.

1.2 Optimal Battery Management

ES and battery based ES in particular, is able to participate in a number of underlying electricity markets aiming to support the modern grid infrastructure. Battery owners therefore need to identify and capture revenue streams from relevant markets to maximize profit.

The electricity market being extremely time sensitive, extensive research has also been invested into optimizing and automating the way batteries participate in one or more markets, using a pool of information relating to the state of supply, demand and network requirements. Knowing when to store and release energy from and to the grid is key to achieving a successful business case for any battery owner, both at the utility MW scale as well as at the domestic kW scale.

Initially, research done on optimizing ES revenue while participating on a certain market has only been incorporating initial fixed battery costs [36], maintenance costs and costs of purchasing energy

during charging phases. However, the importance of considering battery cycle aging when optimizing battery storage control cannot be understated. An excessive number of charge and discharge cycles eventually leads to fatal decrease in battery capacity retention rate.

1.3 Cost of Battery Storage Degradation

The electrochemical nature of battery technology makes it inherently prone to power and energy capacity degradation. The rate at which batteries age is strongly dependent on how they operate over time. It has been shown that certain operating regimes aiming at maximizing profit through energy arbitrage for instance, are applying large amounts of stress onto active battery materials, ultimately reducing capacity retention rates with time. Ignoring the impact of battery operation on aging falsifies long-term profit estimations made by battery owners.

Battery lifetime degradation is a very complex process which is hard to estimate and forecast. Several models of different nature have been proposed in recent years to establish a better perception of long term operating effects on battery life. Better understanding of aging processes, coupled with the increase in accessible battery testing data for various battery technologies has recently allowed researchers to estimate the aging cost component when optimizing battery operation for profit.

Taking battery degradation into account has become a necessary aspect of optimal battery control in most applications, especially when working with MW scale capacities where investment costs remain very substantial.

1.4 Motivation & Report Structure

The objective of this project as a whole, is to delve into the methods of incorporating battery aging costs into for-profit battery control optimization models. This study aims at collecting information and evidence about how battery storage operation impacts capacity fading, for different types of battery technologies. Based on such findings, it becomes possible to consider battery degradation costs to accurately estimate optimal battery control strategies when participating in various electricity markets.

In the Background chapter of the report, the following main points are addressed:

- Generating value through battery storage
- Literature review of optimal battery control considering aging costs
- Literature investigation on different battery technologies

The Aging Cost Model Analysis and Design chapter focuses on:

- Comparing different battery technologies in terms of performance and cycling cost
- Introducing existing degradation models
- Formulating a semi-empirical aging cost model in the context of grid-support applications

The Model Implementation chapter calls upon findings of previous sections to:

- Formulate an optimal bidding strategy model when participating in multiple day-ahead electricity markets
- Incorporate a battery aging cost model into the overall profit maximization model
- Identify and analyze the impact of battery degradation onto the optimal bidding strategy

Chapter 2

Background

2.1 Creating Value with Battery Storage

2.1.1 Overview

Supply Flexibility

ES allows grid operators to easily manage oscillations in supply and demand. The increasing penetration of renewable generation is decreasing overall flexibility of generation due to the intermittent nature of PV and wind generation and the inability to precisely forecast meteorological conditions. ES has the potential to provide additional flexibility by storing excess electricity in times where power output exceeds demand. Similarly, if generation output is lower than expected, ES compensates by injecting the missing power to balance supply and demand.

One thing to note about battery based ES in particular, is its fast response time in the order of a few milli-seconds for some chemistries [4]. This performance ability gives battery based ES the unique advantage of being able to balance supply and demand in real time and with great accuracy.

Accurate and reliable supply of contracted amounts of electricity to customers generates value for generators. Depending on the country of operation, generators receive penalties of varying nature when supply mismatches contracted amounts. In the UK, imbalance prices are used to settle

the difference between contracted generation or consumption and the amount that was actually generated or consumed in each half hour trading period. Under-generation results in generators having to pay for missing energy at a high System-Buy-Price (SBP) [£/MWh]. Over generation however, results in only being able to sell excess energy at low System-Sell-Price (SSP) [£/MWh]. An illustration of two settlement cases are given in Figure 2.1. By virtually isolating themselves from over and under generation through storage, generators are able to offer contracted supply more accurately and generate higher returns.

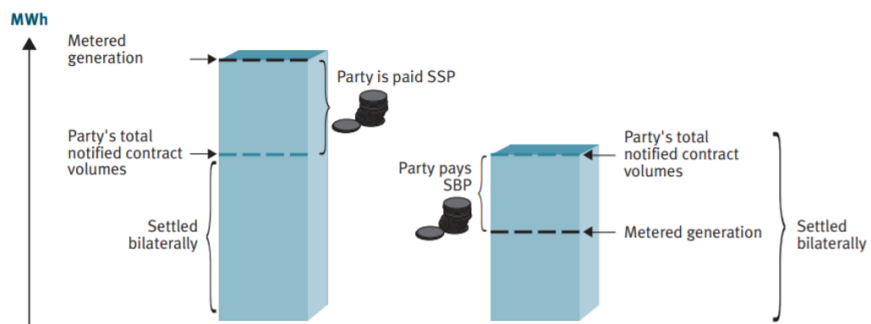


Figure 2.1: Overview of System Sell and System Buy Prices mechanisms

Grid Reliability

According to the Edison Electric Institute, 90% of battery storage capacity installed since 2013 has been deployed by electric companies. ES not only generates value by providing enhanced supply flexibility, but also has immense potential in improving grid reliability by offering services such as:

- Peak load management
- Voltage control
- Frequency control
- Spinning reserves

Overall electricity demand fluctuates significantly throughout the year and even throughout the day (see Figure 2.2). Traditionally, balancing demand in real time and supplying peak load without running out of generation capacity involves using generators such as simple-cycle natural

gas combustion turbines able to start quickly and run for limited times. Peaker plants of this type have very high marginal costs. Large capacity margin and high peak load running costs strongly limits the overall efficiency of supply. When accurately sized for this use case, ES has proven to be a good alternative to the current management of peak load [33]. Through a process known as peak shaving, batteries charge during periods of low demand (usually between 12am and 5am) when electricity prices are low, and deploy electricity at peak load hours (usually between 5pm and 9pm).

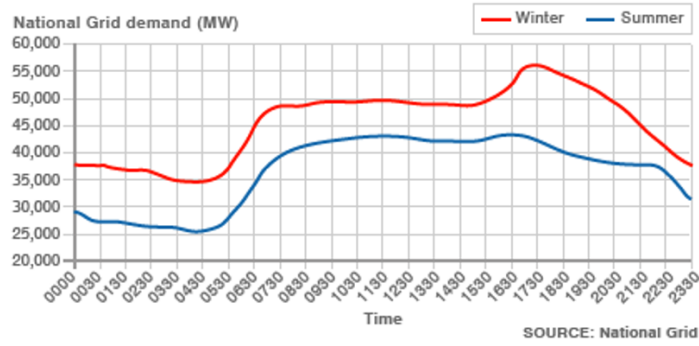


Figure 2.2: Typical summer and winter demands

Third party battery owners also have the possibility to participate in energy arbitrage in an attempt to generate profit. Energy arbitrage consists in purchasing electricity from the grid at low cost and selling it later in the day at high market price driven by peak demand. Peak shaving and energy arbitrage can be illustrated as follows:

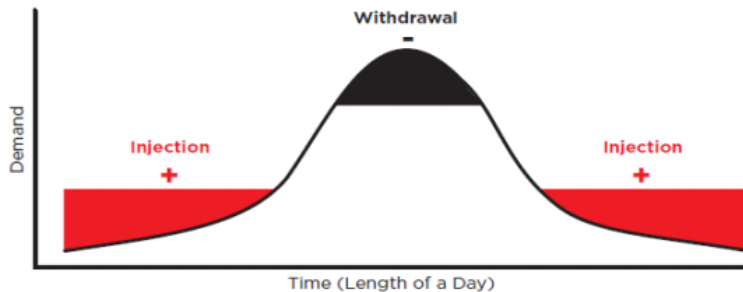


Figure 2.3: Simplified illustration of peak-shaving mechanism

ES is also expected to play a significant role in regulating the frequency of future electric power systems. [50] provides a thorough description of the current landscape of frequency regulation sources

in the UK, highlighting the recent emergence of batteries in providing both reserve and frequency response services. The increasing penetration of renewables also has an impact on the severity of frequency deviation events in a synchronous AC grid system. Imbalances between supply and demand result in deviations from the nominal 50Hz frequency. If demand is in excess of supply, frequency will drop and vice-versa. Frequency should be maintained within statutory (49.5Hz – 50.5Hz) and operational limits (49.8Hz – 50.2Hz) to prevent disconnection of generators and catastrophic failures within the system [18]. Short response times are giving battery based energy storage the possibility to participate in regulating frequency by injecting or absorbing power quickly within the system. For instance, in the UK, enhanced frequency response (EFR) providers are expected to respond to frequency deviations of the network within a second. In return, participants perceive payments based on availability [£/MW/h] [19]. Thanks to its unique response time abilities, ES is able to perceive high returns when participating in EFR.

In July 2016, National Grid purchased a total of 200MW of storage based EFR from seven different providers at a total cost of around 16.25 million pounds per year.

Voltage regulation is crucial to maintain proper operation of connected equipment and generators, facilitate energy transfers, and reduce cable losses. The increased deployment of distributed generation, added to the volatility of connected load is putting certain sections of the grid at risk of significant voltage swings. There are multiple ways of providing voltage support, one of them being to provide (increase voltage) or absorb (decrease voltage) reactive power at a specific busbar to maintain the voltage within nominal range. Once again, battery based ES has proven to be a capable asset in this use case and can provide Enhanced Reactive Power Services (ERPS) to the UK's national grid. If a participant is successfully following the tender assessment, it can perceive payments based on availability [£/MVar/h].

ES can also play a significant role in the reserve capacity market for grid reliability. Generation companies are required to keep generation capacity reserves ready for deployment in a case of plant failure, disruption or large load swings. This precaution is taken to increase security of supply and avoid devastating consequences of blackouts. Electric companies have sometimes found it economically advantageous to deploy ES to help meet or reduce the need for reserve requirements [16]. Reserves are sold guaranteeing the ability to provide continuous power for a set amount of time [£/MW].

Generation Resiliency & Behind the Meter

Generation resiliency is defined by the ability to recover from generation outage or disturbance. Electric companies should have contingency plans to re-energize the grid quickly after a power outage. Battery ES's ability to provide fast response suit the requirements of black start resources used to recover service. Black start corresponds to restoring an electric power station without relying on the power transmission network. Fast response enables minimisation of blackout duration by quickly bringing key fossil-fuelled generators back into operation.

Similarly, ES resources have the potential to isolate a microgrid from power interruptions affecting the main electricity grid. Such use cases allow battery owners to minimize the risk of experiencing extended outages, which would in turn lead to disproportionate financial losses in certain critical applications (industrial, military etc.).

Behind the meter (BTM) applications are also increasingly frequent for battery ES, allowing consumers to maximize benefits of private wind and solar generation and save money through various demand response schemes. Important amounts of research were led in optimising battery operation for kW-scale applications [56][53]. It should however be noted that domestic battery owners are yet to be able to individually participate in utility-scale electricity markets.

2.1.2 Service Comparison

In summary, battery based ES has proven potential to generate value in the following applications:

With Revenues	Without Revenues
Arbitrage	Black Start
Spinning Reserves	Backup Power
Reactive Power	Behind the Meter
Frequency Regulation	

Table 2.1: Value generation methods for battery storage

Increased penetration of renewables and distributed generation is creating growing value for both MW-scale centralised ES and kW-scale domestic ES. However, the scope of this study only encap-

sulates MW-scale applications, involving a broader diversity of battery signals through providing services such as frequency regulation, mostly nonexistent at the domestic level.

Previous studies have demonstrated the necessity to participate in numerous markets in order to generate sufficient returns to justify the application of battery ES. In fact, articles such as [41] have shown that participating in energy arbitrage only does not justify the cost of the batteries when considering degradation. The optimal allocation of resources participating in each market is also crucial to remain competitive [17].

At the MW-scale, it has been shown that providing a combination of energy arbitrage, frequency regulation and reserve services permits reasonably high profits from the perspective of the battery owner. These three activities are kept into consideration for the sake of this study. Two important decision factors helped select these three activities in the context of this project:

1. Prioritizing lucrative activities and markets based on the current market structure.
2. Maintaining broad diversity of battery signal behaviors linked with participation to certain markets.

Participating in energy arbitrage for instance, often translates into charging at night in order to subsequently fully discharge during times of peak demand and high energy prices. This leads to infrequent, deep cycles. Frequency regulation however, is characterized by high frequency cycling, shallow depth of discharge (DOD) and high charging/discharging rates as seen in Figure 2.4 [49]. This contrast enables us to explore various methods of evaluating battery degradation for batteries operating in vastly different ways.

2.2 Literature Review

2.2.1 Optimal Battery Control Considering Battery Aging

The year of 2017 was marked with prominent deployment of utility scale battery storage projects in locations such as California, Australia and Puerto Rico, mostly thanks to the ongoing decrease in energy and power capacity costs over the past 5 to 10 years. A crucial aspect of energy storage investment is to consider limited battery lifetime. Once the initial cost of the battery system is

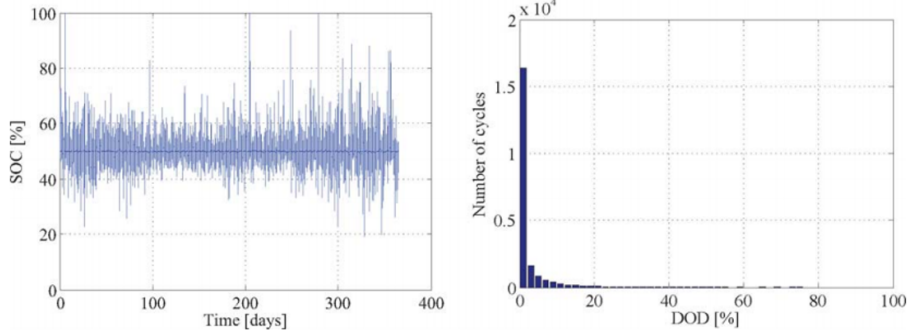


Figure 2.4: Annual state of charge (SOC) profile of battery storage participating in frequency regulation (left) and the corresponding histogram of the number of cycles in function of DOD (right)

covered, costs inherent to the project (connection to the grid, maintenance of infrastructures, among others) only account for around 10% of the total project investment [38]. Battery owners are however facing the necessity to cover their investment and generate profit in a limited time frame, defined by the lifetime of their batteries.

Battery storage owners and operators must employ innovative operating and bidding strategies to secure operational profits against the cost of battery aging [52]. The increasing number of battery storage projects is sourcing valuable information for researchers and operators looking to minimize battery degradation rates and generate higher returns on the long term.

Extensive research efforts have been carried out in recent years to include the aging process in the operation of battery storage, both at the kW and at the MW scale. Reference [10] presents an optimal scheduling model for domestic battery storage, taking the cycling cost into consideration using a method known as Particle Swarm Optimization (PSO). [44] focuses on the US frequency regulation market and proposes online control policy to reduce operation costs and extend battery lifetime. It should be noted that both studies focus of Li-Ion technologies only. Reference [20] investigates the optimal bidding strategy for battery storage in multiple day-ahead power markets, considering the cost of cycle aging and using Vanadium Redox Battery (VRB) technology.

All the publications mentioned in the previous paragraph evaluate cycle aging using a simple depth-of-discharge (DOD) model. Authors of [36], [34] even assume battery fixed lifetime and ignore degradation cost coupled with battery utilization. However, more elaborated semi-empirical aging models have been proposed in [51] for instance. Advanced degradation models are however mostly suited to regular and periodic cycling in experimental conditions, making them unfit for irregular

cycling applications such as e-mobility and grid-support services [44].

Only a very limited amount of publications having a power systems approach to optimal control considering battery aging are looking to overcome the challenge of irregular cycling in order to refine their aging models with more elaborated stress models, corresponding to specific environmental and utilization factors.

2.2.2 Comparative Study of Battery Storage Technologies

Lithium Ion Batteries

Li-Ion batteries are attractive candidates when it comes to participating in MW-scale electricity markets, thanks to long calendar lifetime, low self-discharge rate as well as fast response to name a few [13]. Decreasing manufacturing costs of Li-Ion based batteries are pushing project developers to opt for this type of chemistry more than others. When connected to a load, the potential between the two electrodes (anode and cathode) results in the creation of a current across that load. Electrons are released is Lithium Ions migrate through the electrolyte. A very simplified illustration of the discharging process for a Li-Ion battery is presented in Figure 2.5.

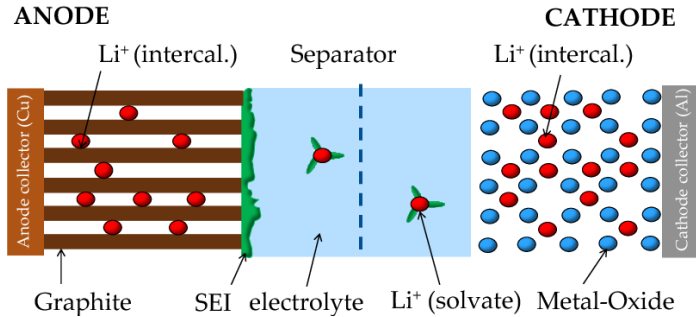


Figure 2.5: High-level diagram of Li-Ion battery operation. [21]

Multiple cathode material options exist in commonly manufactured Li-Ion batteries. These include:

- LCO₂: Lithium Cobalt Oxide
- NMC: Lithium-Nickel Manganese Cobalt Oxide
- NCA: Lithium Nickel Cobalt Aluminium Oxide

- LMO: Lithium Manganese Oxide
- LFP: Lithium Iron Phosphate
- LTO: Lithium Titanate

Each of these battery chemistries have their own benefits and draw backs. While e-mobility applications prioritize high volumetric power and energy densities, grid support applications often require low cost per cycle, fast response and long cycle life at partial cycles. A comparative study of different electrode materials has been issued by [49], suggesting LFP and LTO chemistries bring a number of benefits to the table in a grid-support context, including:

- Low cost
- High intrinsic safety
- Low environmental impact
- High rate charge/discharge capability
- High efficiency (above 90%)

The determination of suitable Li-Ion chemistries is a crucial pre-requisite for the purpose of this project. In fact, this allows gathering of chemistry specific data ultimately improving aging model accuracy.

Lead Acid Batteries

Lead acid technologies are also dominant in the utility scale battery space. Breakthroughs in lead-acid batteries have resulted in the ability to manufacture and deploy lead-acid ES in load balancing and frequency regulation applications [30] at low capital cost. Lead acid batteries have the benefit of being easy to manufacture and reliable.

Lead-acid batteries are however also characterized by their toxic environmental impact and tendency to corrode rapidly which in turns decreases battery efficiency and cycle life. Coulombic efficiency is lower than Li-Ion at around 75%.

An important aspect of rechargeable lead-acid batteries is very limited cycle lifetime, even when using solid lead plates intended to avoid electrode disintegration. Low capital costs justify high cycling degradation rates in backup power and uninterrupted power supply applications, where batteries remain mostly at rest. However, in frequent cycling applications, lead acid batteries are becoming increasingly onerous due to higher cycling costs. [49] justifies this by showing that the cycling cost in €/cycle is 36% higher for lead-acid than for Li-Ion.

Vanadium Redox Batteries

Vanadium redox batteries (VRB) belong to the family of flow batteries. A schematic of a VRB is given in Figure 2.6 [1].

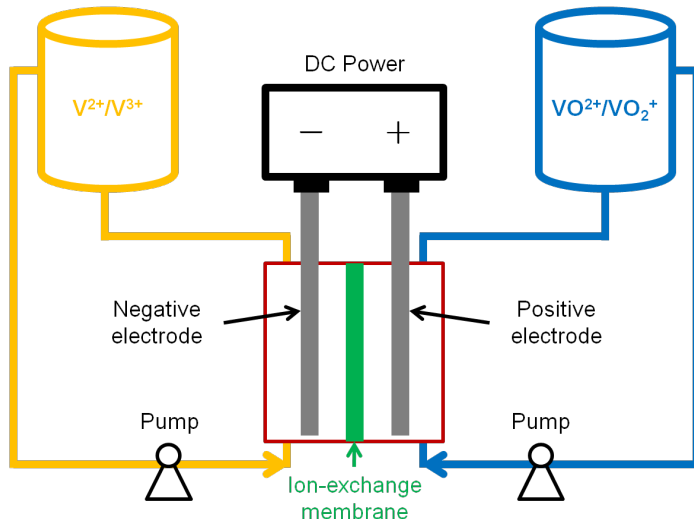


Figure 2.6: High level VRB functional diagram

[22] written by the International Electrotechnical Commission (IEC), gives a good definition of how VRBs operate differently to other solid-state technologies such as Li-Ion:

"In VRBs, two liquid electrolyte dissolutions containing dissolved metal ions as active masses are pumped to the opposite sides of the electrochemical cell. The electrolytes at the negative and positive electrodes are called anolyte and catholyte respectively. During charging and discharging the metal ions stay dissolved in the fluid electrolyte as liquid; no phase change of these active masses takes place. Anolyte and catholyte flow through porous electrodes, separated by a membrane which allows protons to pass through it for the electron transfer process. During the exchange of charge a

current flows over the electrodes, which can be used by a battery powered device. During discharge the electrodes are continually supplied with the dissolved active masses from the tanks; once they are converted the resulting product is removed to the tank.”

Flow batteries in general are characterized by long cycle life partially due to the absence of thermal and mechanical stress during cycling. Efficiency levels are also reasonable at 80% to 87% [15]. VRB’s promising characteristics have been subject to a lot of attention when working in utility-scale bulk ES applications thanks to extended cycle life and reasonable investment costs, provided good maintenance of the system such as refurbishment of stacks and pump components [15].

Lifetime of well-maintained vanadium redox batteries is estimated to reach as much as 15 000 to 20 000 cycles at 100% DOD. It is however important to note that VRB manufacturing costs are currently not experiencing the same decline as Li-Ion technologies, which might affect the competitiveness of VRBs on the long term.

Suitable Chemistry Selection

A number of additional ES methods are actively being considered by researchers to provide grid-support services. These technologies include super capacitors, sodium–sulphur batteries, nickel–cadmium batteries and flywheels. Figure 2.7 provides a visualization of accumulated cycle costs for a year of utilization for each ES technology considered. In appearance, Li-Ion and VRB technologies are considerably cheaper in that perspective than other technologies and are hence chosen as focus points for the remainder of this project.

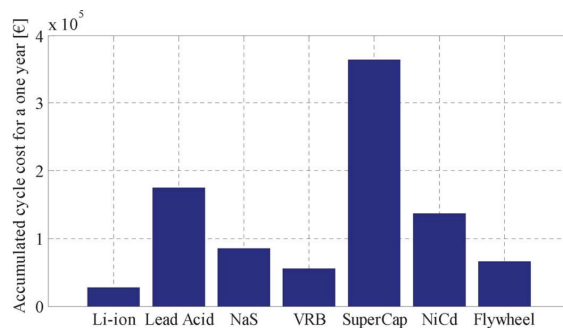


Figure 2.7: Accumulated cycle costs of various ES Technologies

Based on the suitability of both LFP and LTO Li-Ion technologies in grid-support applications, we choose to focus on these two chemistries in particular for Li-Ion.

	LFP	LTO	VRB
Energy Capacity Cost [\$/kWh]	300	3000	210
100% DOD cycle life [no. cycles]	5000	25000	15000
Self-discharge rate [%SOC/month]	1 to 3	1 to 3	-
Energy efficiency [%]	98	92	80 to 87
Main aging process	SEI ¹ formation & Cathode decay	SEI formation & Cathode decay	Battery component aging (pump, cell stack...)
Impact of temperature on lifetime	High	High	Med

Table 2.2: Summary comparison of cost and aging characteristics of LFP, LTO and VRB batteries

A comparison of investment cost and aging characteristics is presented in table 2.2 to further investigate the potential of both Li-Ion and VRB technologies in the context of this project, based on data from [9][5][55].

¹Solid-electrolyte interphase

Chapter 3

Aging Cost Model Analysis & Design

3.1 Battery Storage Degradation Modeling

3.1.1 Introduction to Aging Mechanisms and Modeling

In order to analyse the aging behaviour of the battery for different operating cases, accurate estimation of its degradation behaviour is required. There are multiple methods applied in research and industry to develop battery performance degradation models for all types of chemistries.

In general, battery degradation models can be classified into two types of models: theoretical and empirical. Both approaches vary mainly with respect to the following aspects [8]:

- Complexity of the model
- Purpose of utilization (battery design / circuit simulation / performance evaluation)

Theoretical models include electrochemical models, focusing on the loss of lithium ions alongside other active material degradations in Li-Ion batteries through detailed electrochemical degradation mechanisms [48]. For VRBs, most of the focus is turned towards describing the membrane's degra-

dation [46]. In both cases, most of the battery aging processes are fundamentally dictated by a set of partial differential and algebraic equations [37]. In Li-Ion for instance, the growth of an SEI layer leads to a gradual decrease in cyclable lithium over time [39]. The growth rate of the SEI layer itself due to the accumulation of ethylene bicarbonate is given by:

$$\frac{d\delta}{dt} = - \frac{i_{s,a}}{2F} \frac{M_{SEI}}{\rho_{SEI}}$$

δ is the SEI thickness [m]. $i_{s,a}$ is the side reaction current density at graphite electrode referred to the interfacial surface area of the electrode [A/m^2]. F is faraday's constant. M_{SEI} is the molecular weight of SEI [kg/mol]. ρ_{SEI} is the SEI density [kg/m^3].

C.R. Birk et al. give a more complete list of molecular level degradation mechanisms, their causes, effects and relations to degradation modes in Figure 3.1 [6] for Li-Ion cells. Note that this figure does not take degradation on the battery's kinetics into account (increase in internal resistance), and focuses on cell thermodynamic behaviour (temperature, overpotential etc.).

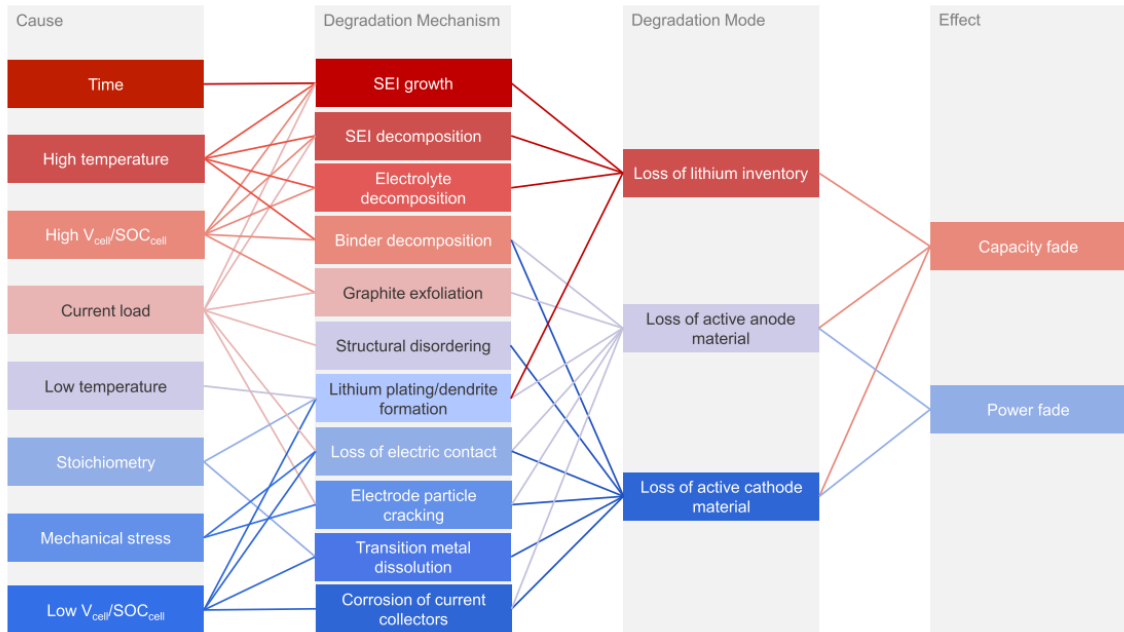


Figure 3.1: Li-Ion molecular level degradation mechanisms, their causes, effects and relations to degradation modes

In real world battery deployment and operation however, it has been argued that correlating

battery charging and discharging with specific molecular-level processes occurring inside each cell lacks in overall accuracy at scale [45][25]. In practice, electrochemical models are predominantly used to optimize battery design at the cell level, regardless of the chemistry at stake [49].

Mathematical modeling of battery cells has been attempted by S.Li and B.Ke in [26]. Mathematical modeling is usually based on a method developed by C. Shepherd in [42] involving a more empirical or stochastic approach. This type of model has however been noticed for its limited modeling accuracy in certain applications [49].

Electrical models are also present in cell design applications. They provide reasonably high modeling accuracy, at the cost of the inability to extrapolate results to other chemistries or cell designs [40]. This is partly because these analytic models, based on a combination of voltage sources, resistors and capacitors are obtained through experimental testing such as DC-pulse testing and EIS-based modeling at the cell level. A basic configuration of a Thevenin-based electrical battery model is given by [49] and shown in Figure 3.2. This model can then be further expanded to take degradation effects into account.

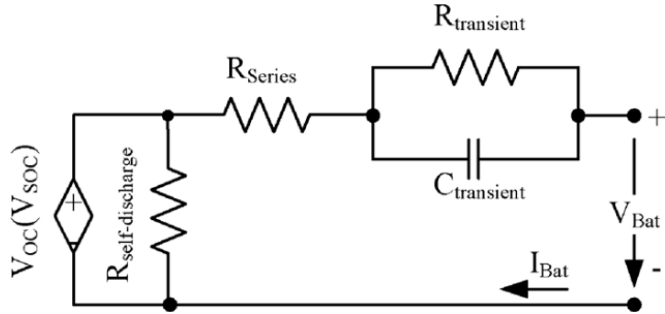


Figure 3.2: Basic configuration of a Thevenin-based electrical battery model [49]

The complexity of those three models coupled with the necessity to adopt and understanding of internal mechanisms to build them, does not allow us to fully incorporate them into the scope of this project. However other simpler empirical models have been suggested, tailored for specific applications such as EV charging and vehicle-to-grid services [32]. The strengths and challenges linked with empirical, theoretical and analytical approaches are summarized in table 3.1.

In our case, providing services of different nature to the grid requires models to be applicable to multiple operating conditions. This can be achieved by calling upon various individual stress models

Approach	Strengths	Drawbacks
Theoretical Models	High precision , Understanding of internal mechanisms	High computational intensity, Needs accurate parametrization
Empirical and Semi Empirical Models	Reasonable accuracy , Low computational intensity	Limited insight into internal cell degradation
Analytic Models	Direct modeling on a pack feasible	Large quantity of experimental data necessary

Table 3.1: Summary of strengths and challenges of degradation models

depending on the battery's operation characteristics. Such a battery life assessment is proposed in [51], de-coupling stress models linked to:

- Number of cycles at a given DOD
- SOC operating region
- Temperature of operation

In MW-scale installations, the impact of temperature on degradation is often assumed negligible as battery installations are usually temperature controlled [20]. We focus on the first two stress models for the sake of this project.

Over the course of our study, each individual stress model is linked to underlying theoretical electrochemical aging processes. This allows for a better understanding of the optimal behavior of battery ES in grid related applications when considering cell degradation.

In practice, the end of life (EOL) criteria for battery ES is such that the battery has reached a 20% capacity fade. An example of degradation curve, showing both experimental points and an empirical aging model, is given in Figure 3.3 [51], showing that EOL is declared after around 3700 cycles for this specific battery chemistry and testing scenario.

3.1.2 DOD Stress Model

DOD stress models are predominantly used to evaluate battery lifetime in a power system context such as ours. At high level, battery capacity degradation is comparable to the fatigue process of

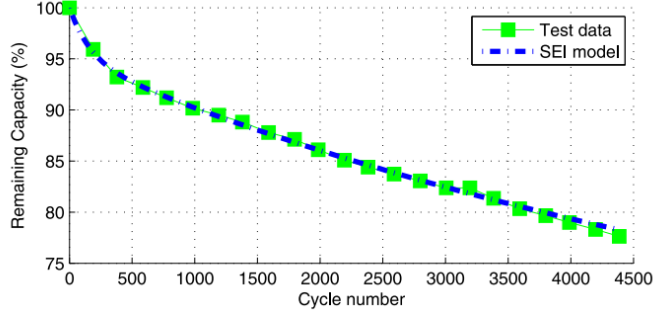


Figure 3.3: An example of Li-Ion degradation curve

materials subject to cyclic loading or stress [24]. Capacity fades according to the depth of each cycle. The maximum number of charge and discharge cycles before failure $f(d)$ as function of depth of discharge d is shown in Figure 3.4, where a deeper cycle stresses batteries significantly more than an equal number of shallower cycles. The shape of the curve, described in part by the value k_p , is dependent on the chemistry and design of battery cells. k_p usually ranges between 0.8 and 1.2 and is normally computed through fitting techniques using data provided by the battery manufacturer and based on empirical field measurements. In most cases in literature, $f(d)$ is expressed as a quadratic function:

$$f(d) = N_{100}^{fail} \times d^{-k_p} \quad (3.1)$$

With N_{100}^{fail} being the maximum number of cycles to failure at 100% DOD.

Other models have been proposed in an attempt to fit aging data of specific chemistries more accurately. An example is given in [51], where three expressions of $f(d)$ are presented and compared for an LMO battery (exponential, quadratic and hybrid models respectively):

$$f_1(d) = kp_{e1} \times d \times e^{kp_{e2} \times d} \quad (3.2)$$

$$f_2(d) = kp_{q1} \times d^{kp_{q2}} \quad (3.3)$$

$$f_3(d) = (kp_{p1} \times d^{kp_{p2}} + kp_{p3})^{-1} \quad (3.4)$$

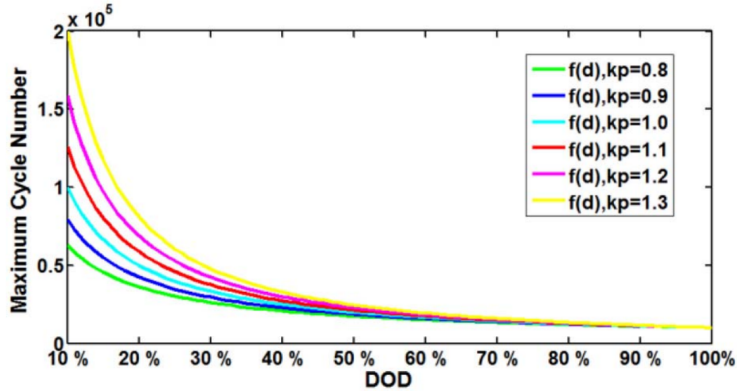


Figure 3.4: Cycle life vs. DOD for different values of k_p

With $k_{p\dots}$ the empirical coefficients obtained experimentally.

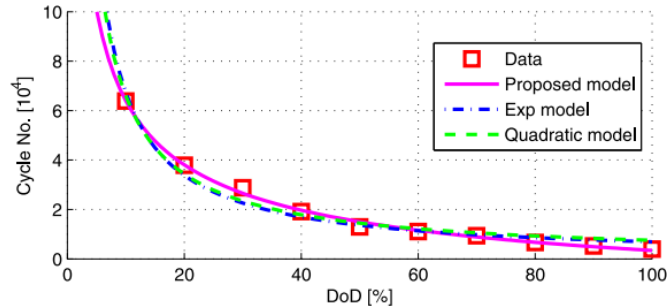


Figure 3.5: Cycle life vs. DOD for different forms of $f(d)$

As can be seen on Figure 3.5, the addition of a supplementary constant value k_{p3} in the proposed hybrid model achieves better fitting of experimental data for this specific LMO battery. We can however observe that the overall improvement in using $f_3(d)$ is not overwhelming and that the quadratic version achieves reasonable fitting of experimental data. The fact that the quadratic form $f_2(d)$ is used extensively in research literature enables us to find chemistry specific empirical coefficient values with more ease and confidence. We therefore choose to keep expressing $f(d)$ in the form of $f_2(d)$, as in equation 3.1.

The model expressed as $f(d)$ provides a convenient one to one mapping between depth of discharge and lifetime, with each cycle causing independent stress. The assumption made when using this model directly is that the battery is subject to constant DOD cycling throughout the entirety

of its lifetime, which is only the case in a very limited amount of uses cases, excluding grid-support applications. In a case where battery participates in frequency regulation, reserves and arbitrage activities, cycle depths are naturally heterogeneous. In order to overcome the challenge of irregular cycling, Yuanyuan Shi et al. have proposed an electrochemically accurate battery capacity-fading model: the rainflow cycle counting degradation model [43]. This algorithm allows counting the number and amplitude of cycles for a heterogeneous material stress profile. This information is then translated into an equivalent number of 100% DOD cycles.

Yuanyuan Shi at al.'s study subsequently call upon that model to solve an optimization problem for optimal battery storage control for frequency regulation, taking degradation into account. The rainflow cycle counting method is often being called upon by researchers with objectives similar to the ones of this study.

The rainflow algorithm is extensively used in general material fatigue analysis [11]. Given a general SOC profile, the algorithm identifies the local extrema corresponding to a change in charging state of the battery, giving information on each charging and discharging half-cycles. The battery completes a half-cycle between each adjacent extreme points.

Let `Rainflow` be the function applying the rainflow counting algorithm on an SOC profile vector \mathbf{x} , we get:

$$\mathbf{d}^{\text{half}} = \text{Rainflow}(\mathbf{x}) \quad (3.5)$$

With \mathbf{d}^{half} , the vector of size K containing each charging and discharging half cycle depths in %. The ASTM E1049-85 version of the rainflow algorithm is chosen in the context of this project.

A simple illustration of the rainflow counting algorithm's output is given in Figure 3.6, taking an arbitrary stress model as input.

The ASTM E1049-85 version of the algorithm was implemented by Piotr Janiszewski in Python [23] and is used in this project to analyze all SOC profile cycling.

Once cycling information (number and amplitude of cycles) is obtained using the rainflow counting algorithm, we look to compute the equivalent number of 100% DOD cycles for \mathbf{x} as a function of \mathbf{d}^{half} and kp . We based our methodology on the one presented in [20].

The cycle life loss for n_d cycles at d DOD is expressed as:

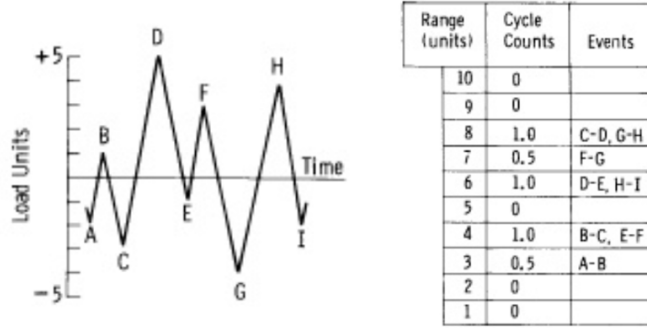


Figure 3.6: Example of rainflow counting algorithm output

$$Loss_{cycle}[\%] = \frac{n_d}{f(d)} \times 100 \quad (3.6)$$

By keeping $Loss_{cycle}$ constant, the equivalent number n_{100}^{eq} of 100% DOD cycles is formulated as:

$$n_{100}^{eq} = n_d \times d^{kp} \quad (3.7)$$

Hence:

$$n_{100}^{eq,day} = \sum_{k \in K} 0.5 \times |d_k^{half}|^{kp} \quad (3.8)$$

For K half cycles identified in the SOC profile using the rainflow counting algorithm.

Note that as kp increases, fewer equivalent 100% DOD cycles are obtained for n_d cycles.

The resulting cycle life T_{cycle} in days is derived as:

$$T_{cycle}[days] = \frac{N_{100}^{fail}}{n_{100}^{eq,day}} \quad (3.9)$$

With $n_{100}^{eq,day}$ computed over a 24h SOC profile.

Similarly, the daily loss of life can then be expressed as:

$$Loss_{cycle}[\%] = \frac{n_{100}^{eq.day}}{N_{100}^{fail}} \times 100 \quad (3.10)$$

Finding chemistry specific values for kp is important for the sake of this study, in order to accurately estimate the daily cycling cost due to battery operation.

According to [12], the kp coefficient for VRB batteries can be set to 0.83 when using our model. For LFP and LTO, we get 0.85 and 0.78 respectively [54].

3.1.3 SOC Stress Model

The SOC stress model is rarely called upon in power system contexts. However, numerous papers such as [14] and [48] stress the important impact of SOC on capacity and power fading. The objective here is describe the stress model linked with the SOC range in which the battery operates in more detail and formulate said model to work alongside the DOD stress model described previously.

In the case of Li-Ion and VRB batteries, terminal voltage decreases as the SOC decreases and vice versa. If batteries are brought close to the extremes or outside of their nominal voltage range, by undercharging or overcharging for instance, this may lead to accelerated degradation rates. The SOC at which a battery operates has an enhancing effect on certain degradation mechanisms in Li-Ion batteries [48]:

High SOC enhances:

- Electrolyte decomposition (Power Fade / Capacity Fade)
- SEI growth (Power Fade)
- Decomposition of binder (Capacity Fade)

Low SOC enhances:

- Current collector corrosion (Power Fade)

The reference SOC value σ_{ref} , where degradation enhancing effects are minimized, is set to 50% [51].

Although low SOC effects are not directly impacting capacity fade, current collector corrosion leads to increased internal resistance and power fade, which in turn affects the battery's lifetime. These effects are however left aside and negligible compared to overpotential effects and in a context where the battery storage tends to not go towards low SOC ranges when providing services such as reserve.

Turning our attention to overpotential (high SOC). Experimental evidence has shown that cycling Li-Ion batteries up to 100% SOC leads to accelerated capacity fading [51]. Figure 3.7 shows experimental results obtained by [29], illustrating the devastating impact of operating the battery in the top 10% of its SOC range.

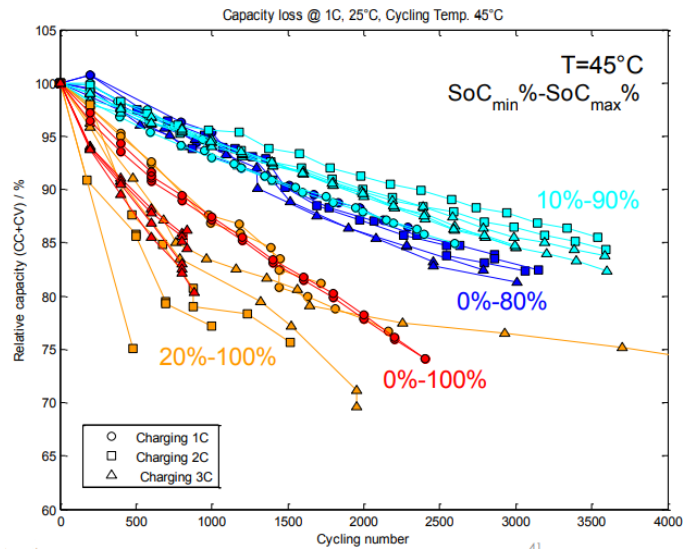


Figure 3.7: Capacity loss of Li-Ion battery for various operating SOC ranges

To incorporate this into a global aging model alongside the DOD stress model, we call upon and re-adapt the model proposed by [51], where high SOC accelerates the degradation rate of the battery. A new expression for n_{100}^{eq} is written as:

$$n_{100}^{eq,day} = \sum_{k \in K} 0.5 \times |d_k^{half}|^{kp} \times \rho \quad (3.11)$$

With $\rho \geq 0$, the accelerating factor due to SOC stress.

To estimate ρ , we adopt the model used in [51], and initially proposed by [31]:

$$\rho = e^{ks(\sigma - \sigma_{ref})} \quad (3.12)$$

With σ the operating SOC, expressed in [%]. This model is in line with the Tafel relationship, an equation in electrochemical kinetics relating the rate of an electrochemical reaction to overpotential, and indicating a higher degradation rate at high SOC levels. ρ 's exponential nature elucidates the high degradation rate at SOCs close to 100%. The value of ks is obtained by fitting ρ to experimental data obtained when cycling at different SOC levels. Contrary to kp values, typical ks values are hard to obtain from existing literature in the time of building this project. No accurate ks^{LTO} value for LTO batteries was found. For LFP batteries, [31] estimates ks^{LFP} to 0.94. In [51], lithium manganese oxide (LMO) batteries have their ks^{LMO} value estimated at 1.04.

With no accurate value for ks^{LTO} , we select a range of plausible values based on the ones found for ks^{LFP} and ks^{LFP} . This range is set to [0.8 : 1.2]. This allows for different values of k^{LTO} to be experimented when testing the model in section 4.4, and a sensibility study is carried out further into the report to analyze the impact of this empirical coefficient on the battery's degradation cost model.

VRB aging mechanisms being very different from the ones of Li-Ion, the same SOC stress model cannot be applied directly to it. Although it has been shown that resistance and side reactions are sometimes a function of SOC in flow batteries, no direct effect on capacity fading was found over the course of this project. Recently, most of the research done in empirical and semi-empirical battery degradation is focusing on Li-Ion chemistries due to their compatibility with the growing e-mobility sector. VRBs are relatively recent inventions characterised by a much lower market penetration compared to Li-Ion. As such literature tends to ignore SOC stress when working with VRBs in power system applications [20].

3.1.4 Calendar Life

An important component of battery lifetime characterization is described by calendar life, otherwise known as shelf life or float life, namely T_{float} expressed in days. For any commodity, shelf life is defined as the length of time said commodity may be stored prior becoming unfit for use, sale or consumption. In the world of battery storage, calendar life is the length of time a battery may be stored (open circuit and at ambient temperature) before reaching EOL. Calendar life is usually in the range of a few years and is very dependent on battery chemistry. For instance, VRB may reach

a calendar life upwards of 20 years, whereas Li-Ion usually reaches EOL after around 10 years of storage, depending on the exact chemistry type. Float life data is usually obtained experimentally and provided by the manufacturer.

3.2 Lifetime Maximization vs. Aging Cost Minimization

Recall that the resulting cycle life T_{cycle} in days can be expressed as in:

$$T_{cycle}[\text{days}] = \frac{N_{100}^{fail}}{n_{100}^{eq.\text{day}}}$$

T_{cycle} is very strongly dependent on the battery's cycling behavior. In certain applications such as e-mobility, the main objective is to extend battery life directly to avoid having to replace the battery very often. In this type of use case, the optimization problem looks to maximize lifetime directly, without necessarily focusing on the cost of replacing the battery once EOL is reached. In that situation, the non-linear optimization problem P_{life} can be expressed as in [20]:

$$P_{life} : \max_{T_{cycle}} (\min(T_{cycle}, T_{float})) \times benefit \quad (3.13)$$

benefit is the reward perceived by the battery's owner when operating the battery in a certain way. This term is necessary in most cases, and justifies battery cycling as opposed to simply remaining at rest to maximize lifetime. Depending on the application, the *benefit* term can be coupled with an income, a performance score or enhanced safety/security.

A limitation to this method for most MW-scale grid applications, is the mismatch between the objective of the problem, to maximize lifetime, and the battery owner's desire to maximize short and long term profit by replacing "expired" batteries without paying attention to the lifetime of batteries.

In order to formulate a more explicit and relevant aging cost model for MW-scale grid-support applications, we focus on the need to maximize profit, without looking to optimize lifetime directly. In idea, degradation losses are mapped to a corresponding financial loss. To achieve this, the aging model is coupled with the cost of replacing the battery once EOL is reached. This method is also used in literature [10]. The formulation of the optimization problem for a given time of operation is

of the form:

$$P_{profit} = \max_{Loss_{cycle}} (income - (Loss_{cycle} \times C_{batt})) \quad (3.14)$$

C_{batt} is the cost of replacing expired battery components. $Loss_{cycle}$ is the loss of cycle life for the given time of operation. $income$ is the income perceived by the battery storage owner for the given time of operation.

In that case, the problem suits an application where batteries are replaced over time. This corresponds to battery owners looking to operate on the long term (10+ years for instance, based on the calendar life of Li-Ion battery ES).

Although both lifetime maximization and cost minimization methods have been used in the context electricity market participation in literature, we choose to work with the latter option. The direct objective to maximize profit by mapping degradation losses to corresponding financial losses justifies this choice. Note however that the two problem formulations are similar as they both depend on the values of $n_{100}^{eq,day}$ and N_{100}^{fail} . The resulting optimal battery operating schemes should be similar in both cases.

A straightforward approach to the consideration of calendar life T_{float} when solving a problem in the form P_{profit} [20], is to introduce it within a hard constraint to the optimization problem:

$$T_{cycle} \leq T_{float}$$

For example, if a battery has a 15 year calendar life, its cycle life resulting from operating in a certain way cannot go beyond that 15 year mark. When optimizing operation on a 24h scale, the equivalent constraint is to force the battery to have a daily loss of cycle life higher or equal to the daily loss of calendar life.

However this reasoning may lead to debatable results. In a case where the optimal battery storage behavior is coupled with a high cycle life, close to T_{float} , setting a hard constraint may be too restrictive. Prices on the electricity market change from one day to the next, and it is reasonable to expect that the battery's optimal behavior may change accordingly. Therefore, as long as $T_{cycle} \leq T_{float}$ is respected, the battery should not be constrained to have a daily loss of cycle life higher or equal to the daily loss of calendar life. In order to give additional freedom to

the battery’s control unit in that perspective, a soft constraint may be used, where the battery is simply “encouraged” to have a high enough daily degradation rate in order to satisfy $T_{cycle} \leq T_{float}$. In the case where optimal cycling behavior results in high cycle aging rates, this modification is unnecessary as the battery will never be in a situation where its daily loss of cycle life is lower than that of calendar life.

In order to enforce the constraint $T_{cycle} \leq T_{float}$, we first start by setting a hard constraint on the loss of cycle life. If the daily loss of cycle life is found to be much higher than the daily loss of calendar life for the optimal operation scheme, the constraint does not need to be modified to a soft one. However if the optimal solution requires that $T_{cycle} \approx T_{float}$, using a soft constraint is preferable.

Chapter 4

Optimal Bidding Strategy Model Considering Cycle Aging Costs

4.1 Markets Operation and Specificities

Basic Market Mechanism

In the context of this project, we are looking to simulate participation to day-ahead energy, spinning reserve and frequency regulation markets. Common settings of electricity markets are implemented in this paper. The model is also developed and programmed in order to accommodate different price dynamics (constant price and hourly-price) and various service portfolios.

Battery ES is assumed to act as a price-taker due to its small capacity compared to other competing generators participating in the same markets. Therefore, battery ES is required to allocate its resources optimally according to market price variations in order to maximize the total expected profit it will generate. A given battery ES storage is able to participate to multiple markets by allocating a certain portion of its total capacity to providing a specific service:

- Cap^{res} is the capacity dedicated to the reserve market [MW].
- Cap^{reg} is the capacity dedicated to the frequency regulation market [MW].

- $Cap^{e.sell}$ is the capacity dedicated to sell on the energy market [MW].
- $Cap^{e.buy}$ is the capacity dedicated to buy on the energy market [MW].

Note that: $Cap^{res} \geq 0$; $Cap^{reg} \geq 0$; $Cap^{e.sell} \geq 0$ and $Cap^{e.buy} \geq 0$

An example of how a 10 MW battery allocates its capacity to provide multiple services is given in Figure 4.1. Note however that a range of operational constraints should be maintained for the rest of the battery, depending on the allocation chosen. These constraints are reviewed further into the report, alongside formulation of the optimisation problem. The bidding strategy has to be established before the closure of the day-ahead markets.

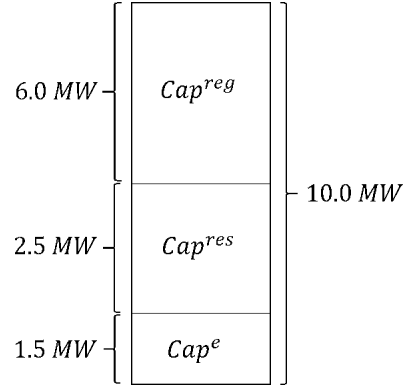


Figure 4.1: Example dispatch for multiple service provision

With $Cap^e = Cap^{e.sell} - Cap^{e.buy}$

Frequency Regulation Service

Frequency regulation services are contracted in various ways depending on the location the system is operating in. In the UK market, payments are perceived based on a long term contract established between National Grid and battery ES owners. The capacity price is constant and participants are penalized if they are unable to accurately respond to the broadcasted frequency regulation signal. In the United-States market, the payment perceived, $Pay^{reg.cap}$, is dependent on both the price of regulation capacity, $P^{reg.cap}$, and the performance of battery, $Score^{perf}$, when it comes to following the FR regulation signal provided by the Regional Transmission Organisation (RTO):

$$Pay^{reg.cap} = P^{reg.cap} Cap^{reg} Score^{perf} \quad (4.1)$$

In this paper, we choose to select a mechanism based on the US model. This is partly justified by the fact that it is more widely used in literature related to this topic. An example of primary frequency response signal is proposed, based on data from [35]. It is shown in Figure 4.2.

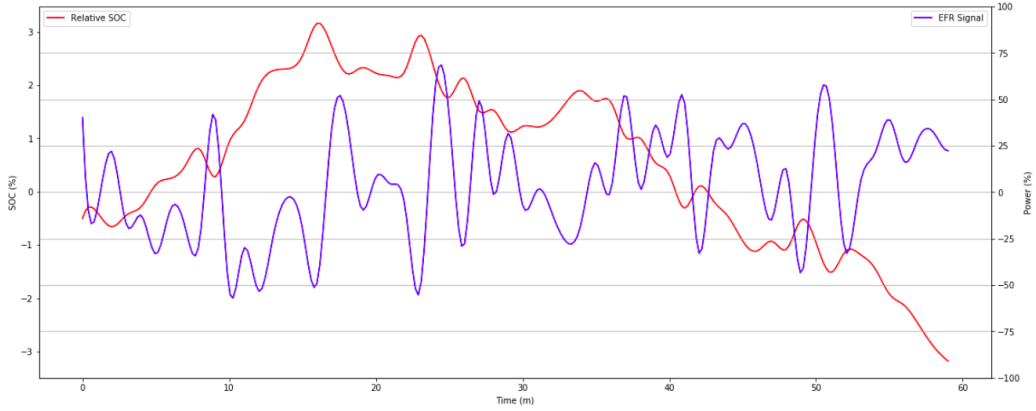


Figure 4.2: 1h EFR Signal and corresponding battery SOC profile

Note that the regulation signal chosen is based off the RegD signal component broadcasted by the PJM RTO in the US. This signal is characterised by high ramp rates, matching the capabilities of both Li-Ion and VRB based ES.

Electricity Market Prices

Day-ahead prices are generated using historical data from two American agencies: PJM and Electric Reliability Council of Texas (ERCOT). Day-ahead prices for energy and reserve services are given by ERCOT, while frequency regulation market prices are issued by PJM. This data illustrates a typical day on the US market and can be considered representative of the average day-ahead price profile. Hourly prices are shown in Figure 4.3, alongside the daily average prices. Note that in that case, prices vary hourly and are very volatile. This suggests that the battery ES's bidding strategy should be revised for every hour.

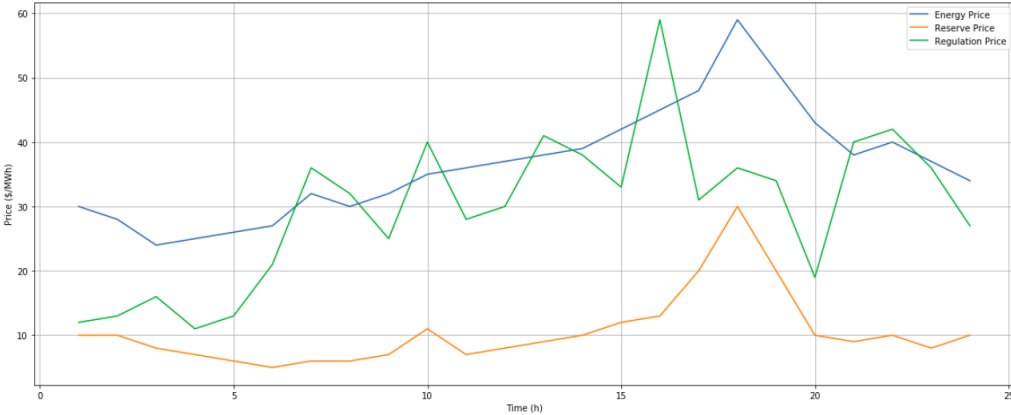


Figure 4.3: Typical day-ahead electricity prices in US dollar

In other markets, such as in the UK, fixed prices are putting less emphasis on the need to re-evaluate capacity dispatch on an hourly basis. In the context of this study, volatile day-ahead prices are enabling us to observe and analyze a more dynamic battery operation scheme over a 24h period, ultimately giving us more insight into the impact of battery aging onto the optimal capacity bidding strategy.

4.2 Formulation of the Optimisation Problem

Objective Function

In the context of this project, we are looking to build a bidding model which maximizes the long term profit of battery storage when participating to three day-ahead markets: the frequency regulation market, the reserves market as well as the energy market. The bidding model is found by solving:

$$\max Profit^{day} = \max \sum_{t \in H} (Income_t^e + Income_t^{res} + Income_t^{reg} - Cost_t^{op}) - Cost_{cycle}^{day} \quad (4.2)$$

With:

H the number of hours in a day.

$Income_t^e$ the net income generated from the energy market during hour t .

$Income_t^{res}$ the income generated from the reserve market during hour t .

$Income_t^{reg}$ the income generated from the frequency regulation market during hour t .

$Cost_t^{op}$ the cost of operating the battery during hour t .

$Cost_{cycle}^{day}$ the equivalent aging cost of operating the battery for a day.

The detailed expressions of $Income_t^e$, $Income_t^{res}$, $Income_t^{reg}$, $Cost_t^{op}$ and $Cost_{cycle}^{day}$ are given further into the report.

The underlying decision variables for this problem are the day-ahead bids of the battery storage for each market for each hour of the day:

$$Cap^{reg} = \begin{bmatrix} Cap_{t=0}^{reg} \\ Cap_{t=1}^{reg} \\ \vdots \\ Cap_{t=23}^{reg} \end{bmatrix} \quad Cap^{res} = \begin{bmatrix} Cap_{t=0}^{res} \\ Cap_{t=1}^{res} \\ \vdots \\ Cap_{t=23}^{res} \end{bmatrix} \quad Cap^{e.sell} = \begin{bmatrix} Cap_{t=0}^{e.sell} \\ Cap_{t=1}^{e.sell} \\ \vdots \\ Cap_{t=23}^{e.sell} \end{bmatrix} \quad Cap^{e.buy} = \begin{bmatrix} Cap_{t=0}^{e.buy} \\ Cap_{t=1}^{e.buy} \\ \vdots \\ Cap_{t=23}^{e.buy} \end{bmatrix}$$

All expressed in MW, giving us a total of $4 \times 24 = 96$ decision variables for this problem.

Incomes

The energy market income has two underlying components, distinct in time: on one hand revenue is perceived from real time reserve deployment, and on the other, from the day-ahead energy bid. The former is always positive. The latter however, can be net positive or net negative, based on the difference between energy sold and energy bought:

$$Income_t^e = P_t^e (Cap_t^{e.sell} - Cap_t^{e.buy})h + P_t^e \gamma^{res} Cap_t^{res} h \quad (4.3)$$

With P_t^e [\$/MWh] the price of energy at time t . h is the duration in hours of the time window of interest and is equal to 1 in our case. γ^{res} denotes the probability of reserve deployment, a factor used in [47].

The reserve market revenue is a linear function of Cap_t^{res} , simply expressed as:

$$Income_t^{res} = P_t^{res} Cap_t^{res} \quad (4.4)$$

With P_t^{res} [\$/MW] the price of reserve capacity at time t.

Finally, the income from frequency regulation services is dependent on the system's ability to follow the operator's regulation signal and is expressed as:

$$Income_t^{reg} = P_t^{reg} Cap_t^{reg} Score^{perf} \quad (4.5)$$

With P_t^{reg} the price of frequency regulation at time t and $Score^{perf} \in [0 : 1]$ the score assigned to battery storage's regulation performance. Reference [20] sets this value to 0.9, thanks to battery storage's ability to provide or absorb large amounts of power almost instantaneously.

Operating Costs

Operating costs are also important to take into account when forecasting expenses linked to a certain battery operating scheme. The cost of operation at hour t is given in [20] as:

$$Cost_t^{op} = c_{op} \times Q_t \quad (4.6)$$

With $Q_t \geq 0$ the amount of total amount of energy change during hour t. c_{op} indicates the operational cost for 1 MWh of energy change in storage.

In our case, Q_t is derived as:

$$Q_t = (Cap_t^{e.sell} + Cap_t^{e.buy})h + 2\beta_t Cap_t^{reg} + \gamma^{res} Cap_t^{res} h \quad (4.7)$$

With β_t the average energy consumed in regulation within hour t for $Cap^{reg} = 1MW$.

Although the operating costs described above depend on the energy change within the battery over time, they do not include any cost related to battery degradation. They are however representative of the variable costs (maintenance, management) linked with charging and discharging the battery and should be included in the overall profit model.

Note however that operational costs are expected to remain relatively small, compared to the costs of degradation. In that case, the optimal solution for profit maximization should prioritize low degradation costs rather than low operational costs.

Battery Costs

Initially, we seek to express the cost $Cost_{batt}$ of replacing batteries after EOL is reached. This cost is crucial in computing the overall profit extracted from battery operation. If $Cost_{batt}$ is large, operation leading to high aging rates will be more penalized than for low $Cost_{batt}$ (assuming identical N_{100}^{fail}).

Initially, we look at the cost of purchasing and installing new battery ES infrastructure. In the case of Li-Ion based batteries (solid state), the battery cost is usually expressed as a function of its capacity in kWh (or sometimes Ah). Note also that the battery's sub-optimal efficiency has to be taken into account: a 90% energy efficient battery able to deliver 1kW for an hour (1kWh), should have a capacity of $1\text{kWh} / 0.9 = 1.1\text{kWh}$. A number of additional costs are usually also added to the cost expression to account for fixed initial costs (transport, installation, construction management, battery management system etc.). Using the cost expression proposed in [49], we compute $Cost_{batt}^{Li-Ion}$ as:

$$Cost_{batt}^{Li-Ion} = \frac{E_{max} \times C_{kWh}}{Eff} + C_f \quad (4.8)$$

In the case of flow batteries such as VRBs, investment costs are expressed differently due to the independence between the energy and power ratings of said batteries. There are three cost sources for VRBs:

- Costs proportional to the energy capacity of the battery [\$/kWh], including cost of electrolyte and electrolyte tanks costs.
- Costs proportional to the power capacity of the battery [\$/kW], including cost of the cell stacks, power conditioning system and pumping systems.
- Fixed costs [\$], including costs of transport, installation, construction management, battery management system etc.

In that sense, [15] argues that the economics of flow batteries are similar to those of other large-scale storage plants, such as pumped hydroelectric facilities or compressed air energy storage (CAES), more than they resemble those of solid state batteries. The investment cost for VRBs is computed as:

$$Cost_{batt}^{VRB} = \frac{E_{max} \times C_{kWh}}{Eff} + \frac{P_{max} \times C_{kW}}{Eff} + C_f \quad (4.9)$$

In the context of this study, we simplify both expressions C_{batt}^{VRB} and C_{batt}^{Li-Ion} by removing the C_f term. This is justified by its low stake in the total battery cost: 7% for VRBs [15], 4% for Li-Ion [3], and by not having to cover a majority of fixed costs when replacing batteries after EOL. Components such as the battery management system for instance do not need to be replaced. New cost expressions are given as:

$$Cost_{batt}^{Li-Ion} = \frac{E_{max} \times C_{kWh}}{Eff} \quad (4.10)$$

$$Cost_{batt}^{VRB} = \frac{E_{max} \times C_{kWh}}{Eff} + \frac{P_{max} \times C_{kW}}{Eff} \quad (4.11)$$

Note that the optimisation problem should consider costs of the battery at the time at which it starts operating, rather than when it needs to be replaced. Aging costs included in the optimal bidding strategy model should be based on the price at which the battery was initially bought.

On the long term however, we can also consider a decrease in the price of batteries over the years, affecting the price of replacement in the future. According to [7] and [1], the price of Li-Ion and VRB batteries should decrease by around 12% and 8%, respectively, on a yearly basis for the next 10 to 20 years. This can be taken into account by introducing a discount factors D^{Li-Ion} or D^{VRB} dependent on the battery's cycle life, resulting in the following expressions:

$$Cost_{batt}^{Li-Ion} = \left[\frac{E_{max} \times C_{kWh}}{Eff} \right] \times D^{Li-Ion} \quad (4.12)$$

$$D^{Li-Ion} = 0.88^{lifeTime}$$

And

$$Cost_{batt}^{VRB} = \left[\frac{E_{max} \times C_{kWh}}{Eff} + \frac{P_{max} \times C_{kW}}{Eff} \right] \times D^{VRB} \quad (4.13)$$

$$D^{VRB} = 0.92^{lifeTime}$$

With *lifeTime* the battery's lifetime in years.

This decrease in price should be considered by investors looking to participate in battery based grid-support activities, as an inevitable decrease in battery storage costs may lead to higher returns, provided electricity market prices are not experiencing the same decline.

Note that for simplicity, we do not consider Net Present Value (NPV) here, as it is beyond the scope of the project. A more accurate battery price forecast would require considering NPV as well.

Aging Costs

Based on expressions 3.14 and 4.2, aging costs for a day of use can be simply expressed as:

$$Cost_{cycle}^{day} = Loss_{cycle}^{day} \times Cost_{batt}^{VRB} \quad (4.14)$$

for VRBs, and:

$$Cost_{cycle}^{day} = Loss_{cycle}^{day} \times Cost_{batt}^{Li-Ion} \quad (4.15)$$

for Li-Ion.

Recall that $Loss_{cycle}^{day}$ is function of $n_{100}^{eq.day}$ and that the SOC stress model is only considered for Li-Ion chemistries in this project. $n_{100}^{eq.day}$'s expression for VRBs and Li-Ion is separated into two components:

$$n_{100}^{eq.day} = n_{100}^{eq.day.FR} + n_{100}^{eq.day.cycle} \quad (4.16)$$

Vanadium Redox Battery:

$n_{100}^{eq.day.cycle}$ is the equivalent daily number of 100% DOD cycles, based on hour to hour SOC changes. Its value is computed using the cycle counting method described in section 3.1.2:

$$n_{100}^{eq.day.cycle}(VRB) = \sum_{k \in C} 0.5 \times |d_k^{half}|^{kp} \quad (4.17)$$

With C the number of half cycles in the hour-to-hour SOC profile.

$n_{100}^{eq.day.FR}$ is the equivalent daily number of 100% DOD cycles, based purely on intra-hour cycling due to frequency regulation. Let $n_{100}^{eq.hour.FR}$ be the hourly number of equivalent 100% DOD cycles in an hour of providing FR at time t . This value is linearly dependent on the dedicated Cap_t^{reg} . As such, a high Cap_t^{reg} value results in deeper frequency regulation cycles. Let $(n_{100}^{eq.hour.FR})_{ref}$ be the equivalent number of 100% DOD cycles for a battery participating only in FR, for the typical cycling profile shown in Figure 4.2:

$$(n_{100}^{eq.hour.FR})_{ref} = \sum_{k \in K} 0.5 \times |d_k^{half}|^{kp} \quad (4.18)$$

With K the number of half cycles in the intra-hour SOC profile. Hence:

$$n_{100}^{eq.day.FR}(VRB) = \sum_{t \in H} \frac{Cap_t^{reg}}{E_{max}} \cdot (n_{100}^{eq.hour.FR})_{ref} \quad (4.19)$$

Li-Ion Battery:

For Li-Ion, we include the SOC stress model by introducing the factor ρ discussed in section 3.1.3. SOC stress is considered when calculating both $n_{100}^{eq.day.FR}$ and $n_{100}^{eq.day.cycle}$. Based on the model expressed in section 3.1.3, we obtain:

$$n_{100}^{eq.day.cycle}(LiIon) = \sum_{k \in C} 0.5 \times \rho_k \times |d_k^{half}|^{kp} \quad (4.20)$$

and

$$n_{100}^{eq.day.FR}(LiIon) = \sum_{t \in H} \frac{Cap_t^{reg}}{E_{max}} \cdot (n_{100}^{eq.hour.FR})_{ref} \cdot \rho_t \quad (4.21)$$

In the equations above, one value of ρ is computed for each hour $t \in [0 : 23]$, based on the battery SOC σ_t using equation 3.12. The relationship between Cap^{reg} , Cap^{res} , $Cap^{e.sell}$, $Cap^{e.buy}$ and the SOC profile is described in the following section.

Operating Constraints

A number of different operating constraints have to be taken into account as we formulate the optimization problem.

Decisions variable boundaries:

Bidding capacities are positive and cannot exceed the maximum power capacity of the battery.

$$0 \leq Cap_t^{e.sell} \leq P_{max}$$

$$0 \leq Cap_t^{e.buy} \leq P_{max}$$

$$0 \leq Cap_t^{res} \leq P_{max}$$

$$0 \leq Cap_t^{reg} \leq P_{max}$$

Recall that: $Cap_t^e = Cap_t^{e.sell} - Cap_t^{e.buy}$

Cap_t^e is the total energy bought or sold on the electricity market at time t . A positive Cap_t^e corresponds to storage selling electricity and vice versa.

Capacity constraints:

The total amount of capacity bids for any hour must remain within lower and upper bounds. For a frequency regulation bid of 1-unit, storage should hold a capacity of ε -units to provide regulation. We obtain the following constraints (lower and upper bound respectively):

$$Cap_t^e - \varepsilon Cap_t^{reg} \geq -P_{max}$$

$$Cap_t^e + Cap_t^{res} + \varepsilon Cap_t^{reg} \leq P_{max}$$

Energy constraints:

When providing ancillary services, battery storage is required to hold energy ready to be deployed according to the needs of the operator. ES should be ready to remain at fully-deployed output for at least h hours for spinning reserves and at least h^{reg} for frequency regulation services [28]. Constraints on the energy level in MWh at hour t (namely E_t) are expressed as:

$$\begin{aligned} E_t &\geq \frac{Cap_t^e h + Cap_t^{res} h + Cap_t^{reg} h^{reg}}{Eff} \\ E_t &\leq E_{max} + (Cap_t^e h - Cap_t^{reg} h^{reg}) \times Eff \end{aligned}$$

State of Charge constraint:

The state of charge at time t is defined in percentage as $\frac{E_t}{E_{max}}$. The value of E_{t+1} is dependent on the value of E_t :

$$E_{t+1} = E_t + \Delta E_t$$

With ΔE_t the change in energy during hour t .

The change in energy is a function of how much energy is being sold, bought and consumed during reserve deployment and losses L^{reg} due to frequency regulation. It can therefore be expressed as:

$$\Delta E_t = -\frac{1}{Eff} \cdot Cap_t^{e.sell} h + Eff \cdot Cap_t^{e.buy} h - \frac{1}{Eff} \cdot \gamma^{res} Cap_t^{res} h - L^{reg}$$

With:

$$L^{reg} = \frac{\beta_t Cap_t^{reg}}{Eff} - Eff \cdot \beta_t Cap_t^{reg}$$

As can be seen in the above expression of L^{reg} , the total loss during regulation up and down during hour t , is the difference between energy discharged and the energy charged from/to the battery. For frequency regulation services, although the regulation signal is assumed to be energy neutral, non-ideal energy efficiency during charging and discharging result in net energy loss.

Finally, we introduce constraint such that the initial and final SOC are equal. In other words, the SOC at the start of the day is equal to the SOC at the end of the day, to avoid having any discontinuity in SOC between each day:

$$E_0 = E_{tmax}$$

With t_{max} the end of the day ($tmax = 23$).

Note that no ramping rate constraint is applied due to fast battery response in the range of a few milliseconds [27], which is negligible compared to the ramp rates of the frequency regulation signal taken into consideration. This assumption is also made in other similar models such as in [20].

4.3 Implementation

Software & High Level Structure

The implementation of models of interest was carried out in Python. Other options were considered such as Matlab and C++. However, Python offers easy array manipulation using the `numpy` library. This library is a useful tool that C++ does not provide. In our case, most of the underlying mathematical expressions involve 1-dimensional arrays. Python also supports another powerful library used to maximize the objective function: the CVXPY optimization library. Provided that the problem definition satisfies a number of conditions, CVXPY provides fast, reliable and stable optimization. CVXPY also has the advantage of calling the solver most specialized to the problem type. The `matplotlib` library and `jupyter lab` IDE provide good, flexible data visualization possibilities. Working in Python instead of Matlab for this project was also a good opportunity to learn how to use industry standard programming methods and tools.

The program's high level structure is illustrated in Figure 4.4.

Working in a `jupyter lab` environment allows to execute each main process of the program sequentially and individually and eases debugging and keeping track of the value of variables. The ability to intercalate markdown between sections of code is also convenient in the context of implementing models.

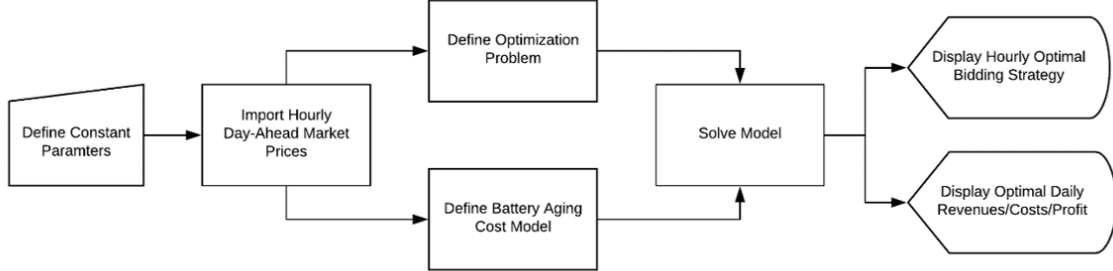


Figure 4.4: High level structure of optimal bidding strategy model

Modular Objective Function

This subsection delves into the inner structure of the processes described in the previous section. In other words, how the optimization problem is built using CVXPY and how the battery aging cost model incorporates decision variables in order to become an integral part of the profit maximization model. In order to avoid having to declare the objective function using decision variables explicitly, which would result in a complex and cumbersome expression, the objective function is broken down into multiple components described in previous sections of this report (incomes, costs etc.). Figure 4.5 illustrates how decision variables are linked with the objective function.

With regards to the definition of the optimization problem, CVXPY offers a very intuitive way of working with large decision variable arrays such as Cap^{res} , $Cap^{e.buy}$, $Cap^{e.sell}$ and Cap^{reg} . This is useful when expressing the income and cost models in a more compact form using array operations directly. For instance, the revenue from the reserve market is defined in one line of code as a 24×1 array (one revenue value per hour), function of Cap^{res} and P^{res} which are both 24×1 arrays. The total revenue for the day, $Income^{res}$, is the sum of elements the resulting array. A similar approach is taken when setting expressions for $Income^{reg}$ and $Income^e$.

Model Flexibility

A significant challenge encountered when implementing the optimal bidding strategy model, was to give it a certain flexibility, given that the model is required to work for multiple battery chemistries, service portfolios and day-ahead market price profiles.

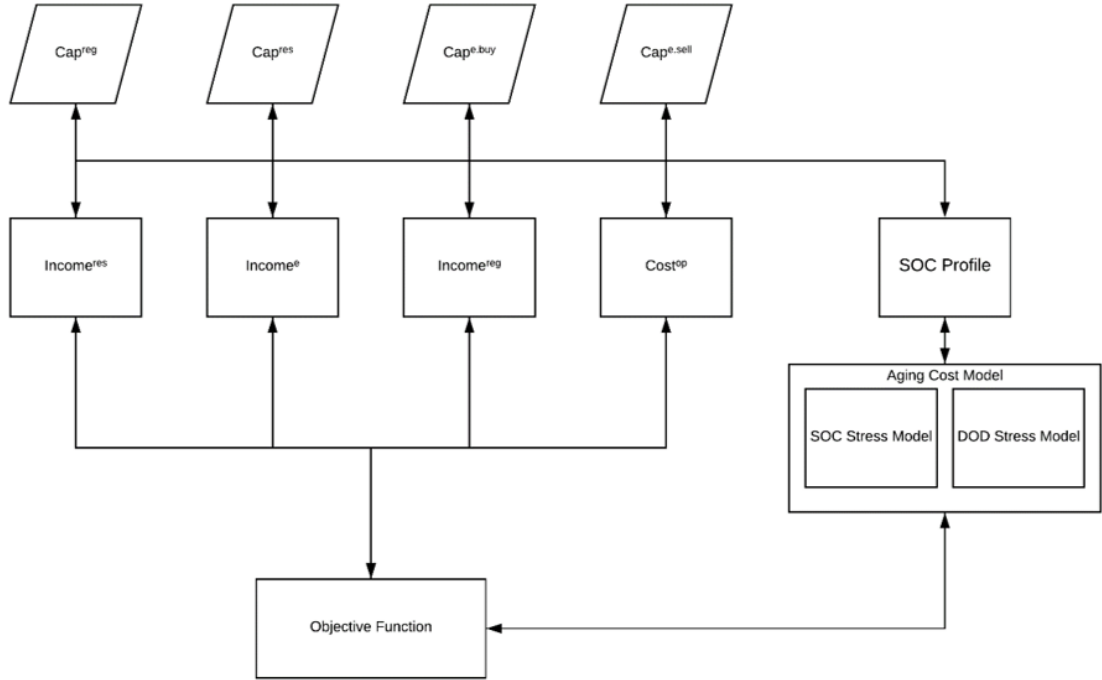


Figure 4.5: Components of the objective function

The Python code starts by initiating default constant parameters, common to all scenarios. Then, the function `setBattParam(BattType)` is called, taking a battery type as input (VRB/LTO/LFP) and assigning the corresponding values to chemistry specific parameters such as N_{100}^{fail} , k_p , E_{eff} etc.. The function also selects the degradation cost model corresponding to the battery type used. Similarly, a function `setPortfolio(PortfolioType)` generates an objective function including all revenue streams unlocked by the portfolio of interest. Note that if the battery provides reserves and/or frequency regulation services, it must also participate in the energy market to buy electricity when needed. Finally, the model should also be capable of operating using different day-ahead market price profiles which may be constant such as in the UK when participating in frequency regulation. A function `importPrices(file)` is used to generate 24×1 vectors containing the day-ahead electricity prices using data stored in external text files.

4.4 Testing and Analysis

Testing Procedure & Default Parameters

A range of parameters are initially selected to build a certain scenario before finding an optimal bidding strategy for the system. These parameters play a key role into finding an optimal bidding strategy. These specific constant parameters are listed below, alongside their default values.

Deployment parameters:

Parameter	Default Value
γ^{res} [%]	5
β_t [MWh/MW]	0.13
h [hours]	1
h^{reg} [hours]	0.25

Storage size parameters:

Parameter	Default Value
P_{max} [MW]	20
E_{max} [MWh]	20
$Score^{perf}$ [%]	90

Maintenance cost parameter:

Parameter	Default Value
c_{op} [\$/MWh]	0.5

Battery specific parameters [2]:

Parameter	LTO	LFP	VRB
Calendar life [years]	20	12	17
C_{kWh} [\$/kWh]	3000	300	210
C_{kW} [\$/kW]	-	-	950
kp	0.78	0.85	0.83
ks	-	0.94	-
Eff [%]	0.98	0.92	0.85
N_{100}^{fail} [cycles]	25000	5000	15000

In order to visualize the impact of battery degradation on the selection of an optimal bidding strategy, the program returns both graphical results describing the hourly bidding strategy for a day, alongside the change in SOC, as well as detailed numerical evidence of optimal revenues, costs and battery aging.

Service Portfolio Analysis for Li-Ion and Vanadium Redox Batteries

In this subsection, we seek to analyze the impact of degradation costs onto the battery's optimal bidding strategy. Assuming participation in all available day-ahead markets (energy, reserves, regulation), the 24 hour optimal bidding strategy for a VRB is illustrated in Figure 4.6, with and without taking aging costs into account.

The corresponding daily revenues, costs and aging data are shown in table 4.1.

In both cases, Figure 4.6 confirms that the battery' optimal bidding strategy is dependent on the price of the day-ahead electricity markets. Regulation capacity dominates for most of the day, thanks to the high payment prices of frequency regulation. However, when regulation prices are comparatively low next to energy prices, especially in the early hours, the battery takes this opportunity purchase electricity and recharge in order to provide frequency regulation later in the day. As the regulation capacity has to be reduced in order for the battery to recharge, the battery turns to the reserve market to keep generating revenues. At around 5pm, the price of regulation is just slightly higher than the price of providing reserves. Again, the battery takes this opportunity to purchase electricity and charge.

Comparing the two optimal bidding strategies, with and without considering aging costs, we notice that the batteries adopt slightly different behaviours. When aging costs are ignored, the battery is subject to deeper cycling, purchasing large amounts of electricity in the early hours

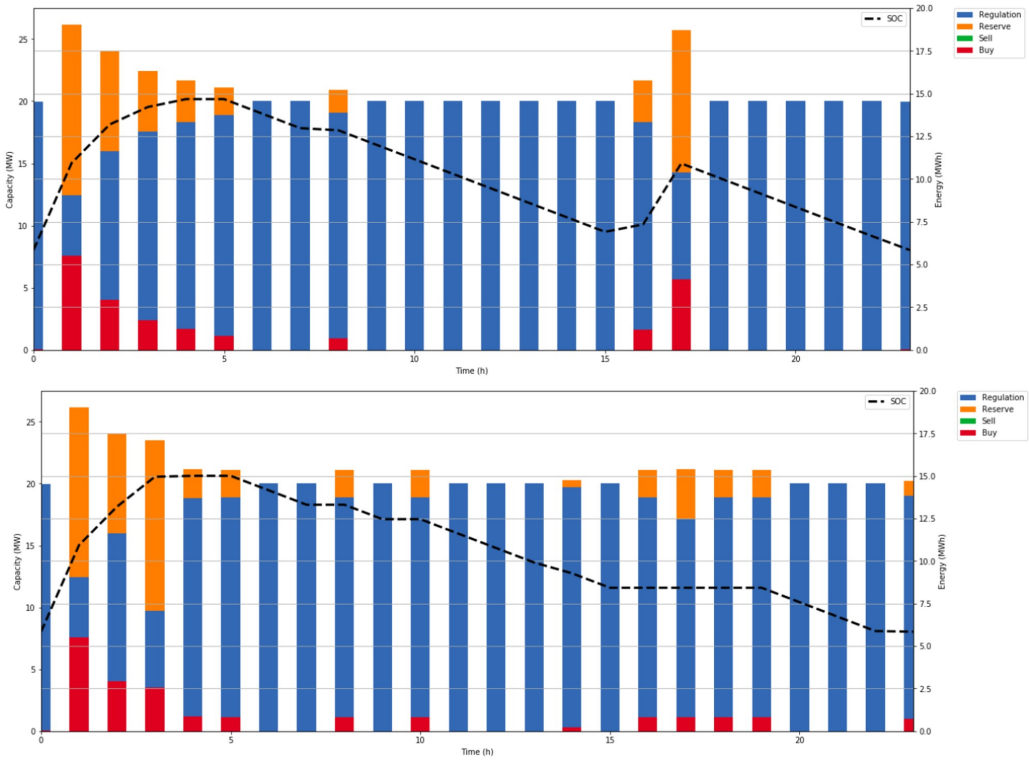


Figure 4.6: Optimal bidding strategies and energy curves of VRB storage. (top) Without consideration of degradation costs, (bottom) with consideration of degradation costs

before participating almost exclusively in frequency regulation services for the rest of the day. The equivalent number of 100% DOD cycles is around 2.84 and the resulting daily aging cost is \$1324. However, when incorporating aging costs into the model, we observe that the battery limits the depth of cycling by avoiding purchasing too much energy early in the day. The battery is also limiting its participation to regulation services having relatively high aging costs associated with them. The resulting number of 100% DOD cycles is lower and aging costs are lowered, leading to overall higher daily profits. The battery's lifetime is also extended by approximatively two years.

The trends and numerical values observed for VRBs are close the ones found in [20], which uses an almost identical bidding model when not considering degradation effects. This allows us to validate the overall optimal bidding strategy model, without including our aging cost model which is different to the one used in that specific paper.

Turning our attention to Li-Ion chemistries, we choose to study the case of LFP, as we know

	Without Aging Cost	With Aging Cost
Regulation Market Income [\\$]	12922	12691
Energy Market Net Income [\\$]	-1001	-940
Reserve Market Income [\\$]	851	927
Operational Costs [\\$]	75	73
100% DOD Equivalent Cycles (Cycling)	0.69	0.42
100% DOD Equivalent Cycles (EFR)	2.15	2.08
Aging Cost [\\$]	1324	1164
Total Profit [\\$]	11373	11439
Estimated Lifetime [years]	14.4	16.3

Table 4.1: Daily revenues, costs and aging data for VRB participating in energy, reserves and regulation markets

exact empirical coefficient values: kp and ks , for its corresponding stress models. The case of LTO will be studied in the following section. The 24h hour optimal bidding strategies with and without aging cost consideration are presented in Figure 4.7.

The corresponding daily revenues, costs and aging data are shown in Table 4.2.

	Without Aging Cost	With Aging Cost
Regulation Market Income [\\$]	13388	13131
Energy Market Net Income [\\$]	-272	-371
Reserve Market Income [\\$]	213	404
Operational Costs [\\$]	67	66
100% DOD Equivalent Cycles (Cycling)	0.44	0.15
100% DOD Equivalent Cycles (EFR)	2.24	2.19
Aging Cost [\\$]	2257	1975
Total Profit [\\$]	11004	11120
Estimated Lifetime [years]	5.0	5.8

Table 4.2: Daily revenues, costs and aging data for LFP participating in energy, reserves and regulation markets

In this case, we note that without taking aging into consideration, the battery focuses only on providing frequency regulation. This is due to Li-Ion's high energy efficiency, giving it a lower

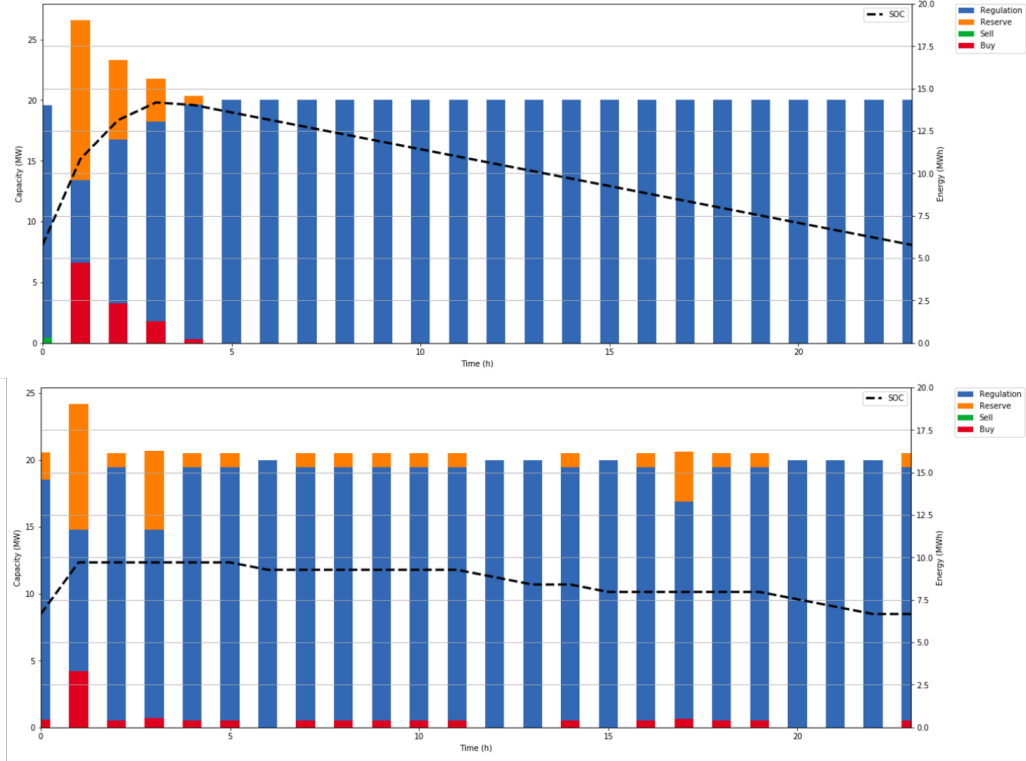


Figure 4.7: Optimal bidding strategies and energy curves of Li-Ion storage. (top) Without consideration of degradation costs, (bottom) with consideration of degradation costs

hourly discharge rate when participating in frequency response. Contrarily to the VRB case, it does not need to purchase supplementary energy during the day to charge. Providing large amounts of frequency regulation does however result in a high number of 100% DOD cycles. When battery degradation costs are being considered, the battery changes strategy and focuses on avoiding large SOC swings by purchasing small amounts of energy throughout the day. The equivalent hour to hour number of 100% DOD cycles is almost divided by four. This however reduces daily regulation market income as the battery tends to participate more in reserve activities. The daily profit is however increased. Note that the frequency regulation is still dominant throughout the day. This can be explained by perceiving regulation payments remaining higher than the aging cost of regulation.

Comparing Li-Ion and VRB profits, we find very similar values. On one hand VRBs have a long cycle life, giving them a much lower daily aging cost than that of Li-Ion batteries. On the other, Li-Ion batteries have better overall performance abilities such as high energy efficiency, allowing them to unlock higher revenues by participating almost exclusively in frequency regulation activities.

Battery cycle lifetime values for both LFP and VRB are significantly lower than their respective float lives. Based on the reasoning discussed in section 3.2, we decide to keep $T_{cycle} \leq T_{float}$ as a hard-constraint and discard the need to use a soft-constraint in that case.

As battery-cycling behaviour differs between frequency regulation, reserve and energy market services, we are interested in analysing the impact of including battery degradation costs for different service portfolios. We consider the following portfolios:

- Energy arbitrage only (Case 1)
- Reserves + Energy purchase (Case 2)
- Frequency regulation + Energy purchase (Case 3)

Figure 4.8 shows optimal bidding strategies for case 1, for both VRB and LFP batteries. For each chemistry, the optimal bidding strategy is identical with and without taking aging costs into account.

For VRB and LFP, we simply observe that the batteries identically participate in energy arbitrage both with and without disregarding aging costs. As expected this involves deep cycling, charging with cheap energy in the morning and selling at a higher price during peak hours. The daily equivalent number of 100% DOD cycles is 0.96 for LFP and 0.92 for VRB, which is also expected. No intra-hour cycling is considered, as batteries are not providing frequency regulation services. Cycling degradation costs are however roughly twice as large as the income made through energy arbitrage. Note that the obtained cycle life is equal to the float life for both chemistries. Hence, when aging costs are taken into account, the behaviour of the battery does not change as it looks to maximize revenues by remaining active during the entirety of its lifetime, even if the net profit is negative. Here we can also introduce a soft constraint on T_{cycle} , as mentioned previously in section 3.2. This initiative gives more freedom to the battery to adopt different arbitrage strategies based on new day-ahead energy prices.

Figure 4.9 shows optimal bidding strategies for case 2 for both VRB and LFP batteries. Once again, for both chemistries, there are no noticeable changes in optimal bidding strategy with and without considering degradation.

Looking at both 24h bidding profiles, we see that the battery charges up with cheap energy in the morning to be able to provide large amounts of reserve during the day. Small amounts of energy

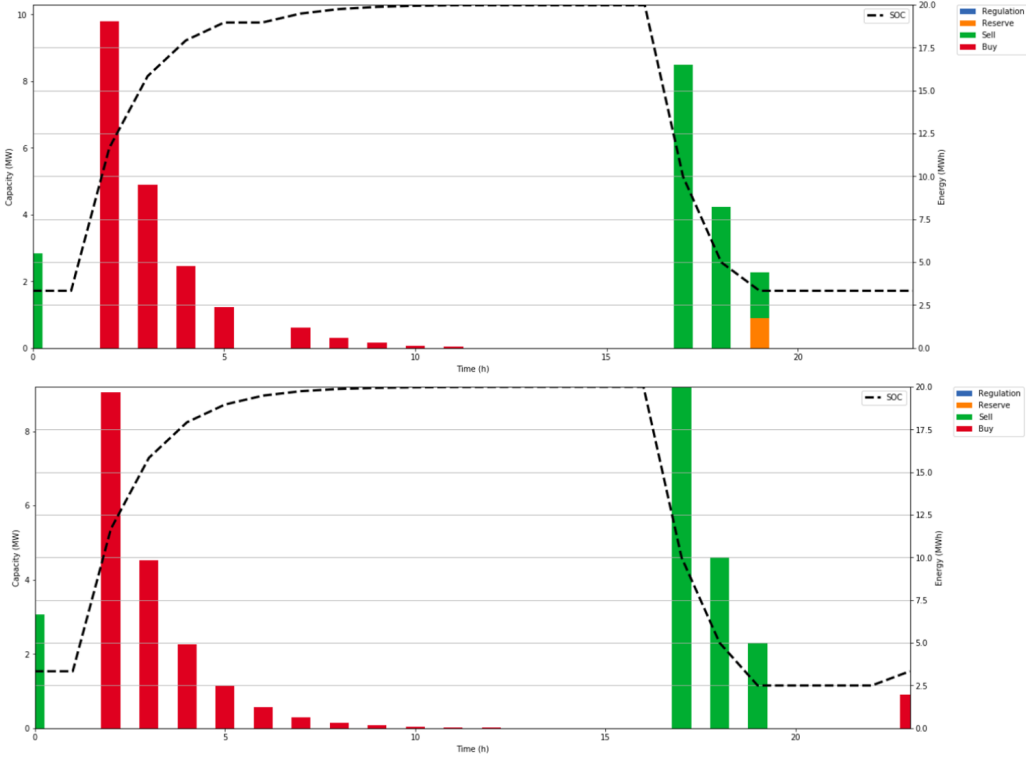


Figure 4.8: Optimal bidding strategies and energy curves of storage when participating to energy arbitrage only. (top) VRB technology (bottom) LFP technology

are purchased throughout the day until the last couple of hours to compensate for deployed energy and to keep generating high reserve income.

For both VRB and LFP, we notice that the battery is providing as much reserve as possible with and without taking degradation into account. Both optimal bidding strategies are almost identical. This can be explained by the fact that providing reserve enables batteries to remain mostly passive leading to negligible degradation costs. As such, the equivalent daily number of 100% DOD cycles is around 0.46 for VRB and 0.39 for LFP. Infrequent and shallow cycling results in lifetime values for both batteries equal to their float life.

The corresponding daily revenues and costs are shown in table 4.3.

Note that low daily aging costs make VRB more profitable assets than LFP batteries when participating to this type of market.

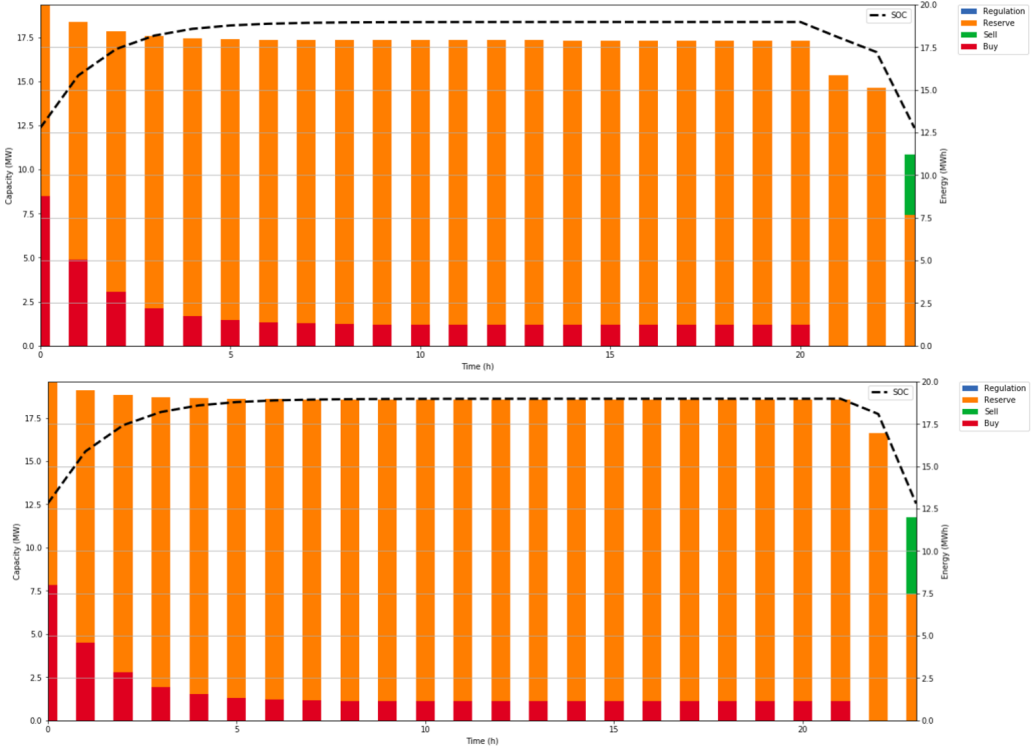


Figure 4.9: Optimal bidding strategies and energy curves of storage when participating to reserves and energy markets. (top) VRB technology (bottom) LFP technology

Finally, we look at case 3. The optimal bidding strategy profiles are given in Figure 4.10.

The corresponding daily revenues and costs are shown in table 4.4:

For VRBs, both optimal bidding profiles show that the battery is looking to maximise the amount of frequency regulation provided throughout the day. When the model ignores aging costs, energy is purchased off the market in the morning during a period of low prices, as well as at around 5pm, when regulation prices are low. This results in a very heterogenous profile as the battery is unable to bid capacity to both charge and provide regulation. Aging costs are very high in this case. When they are considered in the optimal bidding strategy model, we notice that the battery is once again looking to maximize the amount of frequency regulation provided. The profile is however more homogenous, and energy is being purchased regularly throughout the day to avoid deep cycling. As a result, the battery's SOC profiles is kept approximatively constant, close to 50%.

Similar observations are made looking at LFP. Energy is bought exclusively during early hours

	VRB		LFP	
	Without Aging Cost	With Aging Cost	Without Aging Cost	With Aging Cost
Energy Market Net Income [\$]	-319	-319	-318	-318
Reserve Market Income [\$]	4570	4570	4570	4570
Operational Costs [\$]	31	31	31	31
100% DOD Equivalent Cycles (Cycling)	0.46	0.46	0.39	0.39
Aging Cost [\$]	272	272	393	393
Total Profit [\$]	3947	3947	3826	3826
Estimated Lifetime [years]	17	17	12	12

Table 4.3: Daily revenues, costs and aging data for VRB and LFP participating in energy and reserve markets

	VRB		LFP	
	Without Aging Cost	With Aging Cost	Without Aging Cost	With Aging Cost
Regulation Market Income [\$]	13206	12980	12417	12384
Energy Market Net Income [\$]	-653	-752	-256	-281
Operational Costs [\$]	70	70	66	66
100% DOD Equivalent Cycles (Cycling)	0.68	0.11	0.44	0.29
100% DOD Equivalent Cycles (EFR)	2.19	2.19	2.25	2.25
Aging Cost [\$]	3124	2495	1586	1494
Total Profit [\$]	9359	9660	10510	10541
Estimated Lifetime [years]	14	17	5.0	5.3

Table 4.4: Daily revenues, costs and aging data for VRB and LFP participating in energy and regulation markets

when not considering aging costs, whereas energy is bought gradually throughout the day when considering aging costs. For LFP, the change in optimal bidding strategy when considering aging

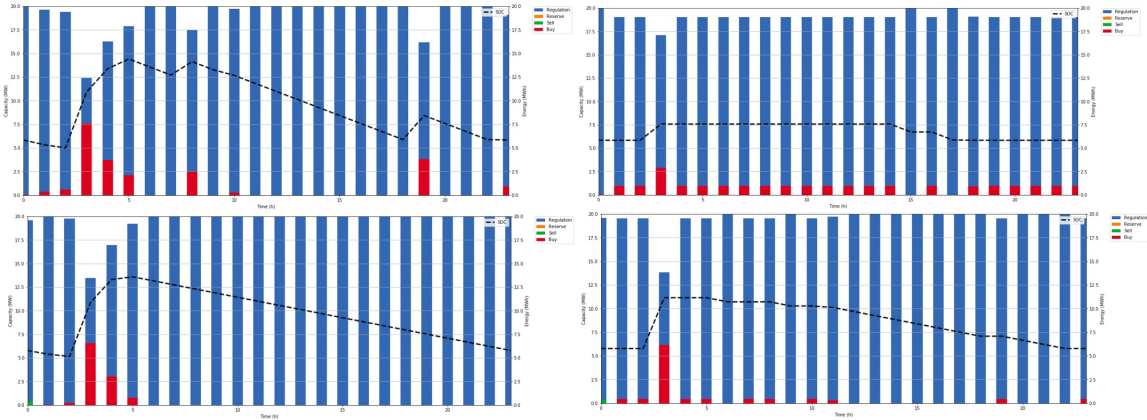


Figure 4.10: Optimal bidding strategies and energy curves of storage when participating to regulation and energy market. (top left) VRB technology without aging cost consideration (top right) VRB technology with aging cost consideration (bottom left) LFP technology without aging cost consideration (bottom right) LFP technology with aging cost consideration

costs is not as significant as for VRB. Looking at the data presented in table 4.4, we notice that battery lifetime and overall profits are subject to very slight increase. Based on observations, higher energy efficiency is making LFP a more profitable asset than VRB when participating in frequency regulation only.

SOC Stress Sensibility Study

Turning our attention to the LTO battery SOC stress model, we are interested in observing the impact of the value of k_s when computing the ρ factor used in aging cost estimation. No clear k_s^{LTO} value was found in literature to work with our model. The lack of experimental data does not give us the possibility to find k_s^{LTO} empirically using a chemistry specific capacity fade profile. As mentioned in section 3.1.3, we choose to select a range of plausible values for k_s^{LTO} , based on other k_s values found for similar chemistries such as LMO and LFP. The chosen range is [0.8 : 1.2]. Initially, we are interested in the optimal bidding strategy found without taking aging costs into consideration for LTO battery storage, given in Figure 4.11:

We notice that LTO's very high energy efficiency results in low net discharge rates when providing frequency regulation. The battery is therefore almost entirely focusing on frequency regulation services and only needs to purchase small amounts of energy throughout the day. We can also

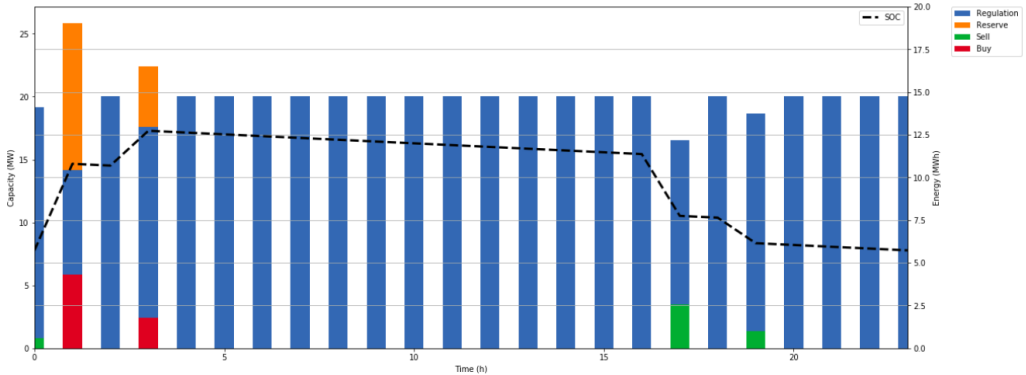


Figure 4.11: Optimal bidding strategies and energy curve of LTO battery storage when participating to reserves, regulation and energy markets without aging costs consideration

observe a hint of energy arbitrage activity, as energy is sold at around 5pm, where electricity prices are high and regulation prices drop.

When aging costs are incorporated into the model, the optimal bidding profiles are shown in Figure 4.12.

Looking at all three profiles, we notice that the battery is aiming at operating at constant SOC throughout the day to minimize hour to hour cycle depth. As the value of ks^{LTO} increases, the battery is looking to operate at a lower SOC in order to limit degradation costs linked with SOC stress. In order to achieve this, the battery purchases slightly less energy during the day. Just enough energy is purchased to keep the SOC constant. Thankfully, high energy efficiency minimizes the amount of energy purchased during the day. In terms of daily profit, we obtain \$ 9558, \$ 9514 and \$ 9462 for ks^{LTO} equal to 0.8, 1, 1.2 respectively. As the ks factor increases, the battery is encouraged to decrease its operating SOC and provide frequency regulation in times where regulation prices are comparatively low. Note that the difference in profits remains very small.



Figure 4.12: Optimal bidding strategies and energy curve of LTO battery storage when participating to reserves, regulation and energy markets with aging costs consideration (top) $ks = 0.8$, (middle) $ks = 1$, (bottom) $ks = 1.2$

Chapter 5

Conclusion & Future Work

In conclusion, it has been shown that although battery storage has a proven potential to compete on numerous electricity markets by providing various grid-support services, significant lifetime limitations impose an important cost for battery ES owners and investors. It has become necessary for battery operators to integrate the costs of battery degradation into their profit forecast. Both VRB and Li-Ion technologies are studied throughout this project, thanks to their suited characteristics for grid-support applications and low cycling costs compared to other battery chemistries.

The correlation between battery operation and degradation rate is depicted in the context of MW-scale grid-support activities. A semi-empirical aging model is proposed, drawing from existing literature using a power system level approach, as well as articles delving into individual degradation causes and effects at the cell level. The proposed model calls upon a cycle counting algorithm to overcome the challenges imposed by irregular cycling. The obtained degradation model is then transformed into an aging cost model. Ultimately, two different aging cost models are formulated, one being tailored to certain Li-Ion chemistries, the other suited for VRBs. In order to visualize the impact of battery degradation costs on optimal battery control for different market activities and battery technologies, the aging cost model is incorporated into an optimal bidding strategy model for day-ahead market participation, involving ancillary services such as reserves and frequency regulation, but also considering participation on the electricity wholesale market. Testing the resulting model for both Li-Ion and VRBs has shown that the optimal hourly bidding strategy re-adapts itself when considering battery storage degradation costs, in order to strike the optimal balance between degradation rate and revenue generation. A portfolio study gave us an understanding as to how

certain specific services affect battery lifetime and whether or not profit can be generated when considering aging costs. Additional contrast is brought to the study by comparing aging effects on two very different battery technologies currently gathering noteworthy attention in the context of grid-support applications.

An important limitation to this project is the validation of the aging cost models. Empirical coefficients chosen throughout this study are selected from literature. Although these coefficients are chemistry specific and seem to generate coherent results based on the implemented optimal bidding strategy model, they should be re-evaluated or validated using more precise experimental data which could not be obtained over the course of this project. Coefficients can subsequently be computed using curve fitting methods extensively discussed in literature. The model's accuracy could therefore be refined in the future by gaining access to relevant degradation related experimental data.

Another future path of exploration for this project would be to incorporate aging costs into an online optimal bidding strategy model, in order to operate in activities requiring real-time control decision making such as for domestic applications. The research carried out in this project is focusing on participation to day-ahead markets, where market prices are estimations based on historical data and capacity dispatch is made one day in advance. Designing an online optimization model would require a different approach involving a mix of historical data and heuristic models.

Bibliography

- [1] Improving the performance and reducing the cost of vanadium redox flow batteries for large-scale energy storage.
- [2] Piergiorgio Alotto, Massimo Guarneri, and Federico Moro. Redox flow batteries for the storage of renewable energy: A review. *Renewable and Sustainable Energy Reviews*, 29:325–335, 2014.
- [3] David Anderson. An evaluation of current and future costs for lithium-ion batteries for use in electrified vehicle powertrains. 2009.
- [4] Riyanto Trilaksono Bambang, Arief Syaichu Rohman, Cees Jan Dronkers, Romeo Ortega, Arif Sasongko, et al. Energy management of fuel cell/battery/supercapacitor hybrid power sources using model predictive control. *IEEE Transactions on Industrial Informatics*, 10(4):1992–2002, 2014.
- [5] Anthony Barré, Benjamin Deguilhem, Sébastien Grolleau, Mathias Gérard, Frédéric Suard, and Delphine Riu. A review on lithium-ion battery ageing mechanisms and estimations for automotive applications. *Journal of Power Sources*, 241:680–689, 2013.
- [6] Christoph R Birkl, Matthew R Roberts, Euan McTurk, Peter G Bruce, and David A Howey. Degradation diagnostics for lithium ion cells. *Journal of Power Sources*, 341:373–386, 2017.
- [7] BNEF. Lithium-ion battery costs and market.
- [8] Min Chen and Gabriel A Rincon-Mora. Accurate electrical battery model capable of predicting runtime and iv performance. *IEEE transactions on energy conversion*, 21(2):504–511, 2006.
- [9] Daiwon Choi, Wei Wang, Vish V Viswanathan, and Gary Z Yang. Low cost, long cycle life, li-ion batteries for stationary applications. *DOE EERE Energy Storage Program Annual Update 2010*, 2010.

- [10] Carlos Adrian Correa, Alexis Gerossier, Andrea Michiorri, and Georges Kariniotakis. Optimal scheduling of storage devices in smart buildings including battery cycling. In *PowerTech, 2017 IEEE Manchester*, pages 1–6. IEEE, 2017.
- [11] Stephen D Downing and DF Socie. Simple rainflow counting algorithms. *International journal of fatigue*, 4(1):31–40, 1982.
- [12] Rodolfo Dufo-López, José L Bernal-Agustín, and José A Domínguez-Navarro. Generation management using batteries in wind farms: Economical and technical analysis for spain. *Energy policy*, 37(1):126–139, 2009.
- [13] Bruce Dunn, Haresh Kamath, and Jean-Marie Tarascon. Electrical energy storage for the grid: a battery of choices. *Science*, 334(6058):928–935, 2011.
- [14] Bruce Dunn, Haresh Kamath, and Jean-Marie Tarascon. Electrical energy storage for the grid: a battery of choices. *Science*, 334(6058):928–935, 2011.
- [15] S Eckroad. Vanadium redox flow batteries: an in-depth analysis. *Electric Power Research Institute, Palo Alto, CA*, 1014836, 2007.
- [16] Jim Eyer and Garth Corey. Energy storage for the electricity grid: Benefits and market potential assessment guide. *Sandia National Laboratories*, 20(10):5, 2010.
- [17] TENG Fei and Goran Strbac. Business cases for energy storage with multiple service provision. *Journal of Modern Power Systems and Clean Energy*, 4(4):615–625, 2016.
- [18] DM Greenwood, Khim Yan Lim, C Patsios, PF Lyons, Yun Seng Lim, and PC Taylor. Frequency response services designed for energy storage. *Applied Energy*, 203:115–127, 2017.
- [19] National Grid. Enhanced frequency response market information report. 2016.
- [20] Guannan He, Qixin Chen, Chongqing Kang, Pierre Pinson, and Qing Xia. Optimal bidding strategy of battery storage in power markets considering performance-based regulation and battery cycle life. *IEEE Transactions on Smart Grid*, 7(5):2359–2367, 2016.
- [21] Holger C Hesse, Michael Schimpe, Daniel Kucevic, and Andreas Jossen. Lithium-ion battery storage for the grid—a review of stationary battery storage system design tailored for applications in modern power grids. *Energies*, 10(12):2107, 2017.
- [22] International Electrotechnical Comission (IEC). Electrical energy storage.

- [23] Piotr Janiszewski. Astm e1049-85 python implementation. [<https://github.com/iamlikeme/rainflow>; Online; accessed 9-June-2018].
- [24] Izaro Laresgoiti, Stefan Käbitz, Madeleine Ecker, and Dirk Uwe Sauer. Modelling mechanical degradation in lithium-ion batteries during cycling. In *Meeting Abstracts*, number 5, pages 356–356. The Electrochemical Society, 2014.
- [25] Izaro Laresgoiti, Stefan Käbitz, Madeleine Ecker, and Dirk Uwe Sauer. Modeling mechanical degradation in lithium ion batteries during cycling: Solid electrolyte interphase fracture. *Journal of Power Sources*, 300:112 – 122, 2015.
- [26] Shuhui Li and Bao Ke. Study of battery modeling using mathematical and circuit oriented approaches. In *Power and Energy Society General Meeting, 2011 IEEE*, pages 1–8. IEEE, 2011.
- [27] Xing Luo, Jihong Wang, Mark Dooner, and Jonathan Clarke. Overview of current development in electrical energy storage technologies and the application potential in power system operation. *Applied Energy*, 137:511–536, 2015.
- [28] Ralph D Masiello, Brad Roberts, and Tom Sloan. Business models for deploying and operating energy storage and risk mitigation aspects. *Proceedings of the IEEE*, 102(7):1052–1064, 2014.
- [29] Ecole D'ingenieurs La Rochelle Mat4Bat Summer School. Cycling aging of lithium-ion batteries. 2015.
- [30] Brian B McKeon, Jun Furukawa, and Scott Fenstermacher. Advanced lead-acid batteries and the development of grid-scale energy storage systems. *Proceedings of the IEEE*, 102(6):951–963, 2014.
- [31] Alan Millner. Modeling lithium ion battery degradation in electric vehicles. In *Innovative Technologies for an Efficient and Reliable Electricity Supply (CITRES), 2010 IEEE Conference on*, pages 349–356. IEEE, 2010.
- [32] Miguel A Ortega-Vazquez. Optimal scheduling of electric vehicle charging and vehicle-to-grid services at household level including battery degradation and price uncertainty. *IET Generation, Transmission & Distribution*, 8(6):1007–1016, 2014.
- [33] Alexandre Oudalov, Rachid Cherkaoui, and Antoine Beguin. Sizing and optimal operation of battery energy storage system for peak shaving application. In *Power Tech, 2007 IEEE Lausanne*, pages 621–625. IEEE, 2007.

- [34] Hrvoje Pandžić, Yishen Wang, Ting Qiu, Yury Dvorkin, and Daniel S Kirschen. Near-optimal method for siting and sizing of distributed storage in a transmission network. *IEEE Transactions on Power Systems*, 30(5):2288–2300, 2015.
- [35] PJM. Regulation signal and requirement update pjm.
- [36] Junjie Qin, Yinlam Chow, Jiyan Yang, and Ram Rajagopal. Online modified greedy algorithm for storage control under uncertainty. *IEEE Transactions on Power Systems*, 31(3):1729–1743, 2016.
- [37] Venkatasailanathan Ramadesigan, Paul WC Northrop, Sumitava De, Shriram Santhanagopalan, Richard D Braatz, and Venkat R Subramanian. Modeling and simulation of lithium-ion batteries from a systems engineering perspective. *Journal of The Electrochemical Society*, 159(3):R31–R45, 2012.
- [38] Ana Rodrigues, Denise Machado, and Tomaz Dentinho. Electrical energy storage systems feasibility; the case of terceira island. *Sustainability*, 9(7):1276, 2017.
- [39] M Safari and C Delacourt. Simulation-based analysis of aging phenomena in a commercial graphite/lifepo₄ cell. *Journal of The Electrochemical Society*, 158(12):A1436–A1447, 2011.
- [40] Dirk Uwe Sauer and Heinz Wenzl. Comparison of different approaches for lifetime prediction of electrochemical systems—using lead-acid batteries as example. *Journal of Power sources*, 176(2):534–546, 2008.
- [41] Anastasia Shcherbakova, Andrew Kleit, and Joohyun Cho. The value of energy storage in south korea’s electricity market: A hotelling approach. *Applied energy*, 125:93–102, 2014.
- [42] Clarence M Shepherd. Design of primary and secondary cells ii. an equation describing battery discharge. *Journal of the Electrochemical Society*, 112(7):657–664, 1965.
- [43] Yuanyuan Shi, Bolun Xu, Yushi Tan, and Baosen Zhang. A convex cycle-based degradation model for battery energy storage planning and operation. *arXiv preprint arXiv:1703.07968*, 2017.
- [44] Yuanyuan Shi, Bolun Xu, and Baosen Zhang. Optimal battery control under cycle aging mechanisms. *arXiv preprint arXiv:1709.05715*, 2017.
- [45] Kandler Smith, E Wood, S Santhanagopalan, GH Kim, J Neubauer, and A Pesaran. Models for battery reliability and lifetime. Technical report, National Renewable Energy Laboratory (NREL), Golden, CO., 2014.

- [46] Ao Tang, Jie Bao, and Maria Skyllas-Kazacos. Dynamic modelling of the effects of ion diffusion and side reactions on the capacity loss for vanadium redox flow battery. *Journal of Power Sources*, 196(24):10737–10747, 2011.
- [47] Ali Karimi Varkani, Ali Daraeepour, and Hassan Monsef. A new self-scheduling strategy for integrated operation of wind and pumped-storage power plants in power markets. *Applied Energy*, 88(12):5002–5012, 2011.
- [48] J Vetter, P Novák, MR Wagner, C Veit, K-C Möller, JO Besenhard, M Winter, M Wohlfahrt-Mehrens, C Vogler, and A Hammouche. Ageing mechanisms in lithium-ion batteries. *Journal of power sources*, 147(1-2):269–281, 2005.
- [49] M Wierczyski, D Ioanstroe, A Stan, R Teodorescu, and D Uwe Sauer. Selection and performance-degradation modeling of limo/li ti o and lifepo/c battery cells as suitable energy storage systems for grid integration withwind power plants: An example for the primary frequency regulation service. *IEEE Transactions on Sustainable Energy*, 5(1), 2014.
- [50] Heather Wyman-Pain, Yuankai Bian, Cain Thomas, and Furong Li. The economics of different generation technologies for frequency response provision. *Applied Energy*, 222:554–563, 2018.
- [51] Bolun Xu, Alexandre Oudalov, Andreas Ulbig, Goran Andersson, and Daniel Kirschen. Modeling of lithium-ion battery degradation for cell life assessment. *IEEE Transactions on Smart Grid*, 2016.
- [52] Bolun Xu, Yuanyuan Shi, Daniel S Kirschen, and Baosen Zhang. Optimal battery participation in frequency regulation markets. *arXiv preprint arXiv:1710.10514*, 2017.
- [53] Z. Xu, X. Guan, Q. S. Jia, J. Wu, D. Wang, and S. Chen. Performance analysis and comparison on energy storage devices for smart building energy management. *IEEE Transactions on Smart Grid*, 3(4):2136–2147, Dec 2012.
- [54] Bo Yang, Yuri Makarov, John Desteeese, Vilayanur Viswanathan, Preben Nyeng, Bart McManus, and John Pease. On the use of energy storage technologies for regulation services in electric power systems with significant penetration of wind energy. In *Electricity Market, 2008. EEM 2008. 5th International Conference on European*, pages 1–6. IEEE, 2008.
- [55] Cheng Zhang, TS Zhao, Qian Xu, Liang An, and Gang Zhao. Effects of operating temperature on the performance of vanadium redox flow batteries. *Applied Energy*, 155:349–353, 2015.

- [56] Menglian Zheng, Christoph J Meinrenken, and Klaus S Lackner. Smart households: Dispatch strategies and economic analysis of distributed energy storage for residential peak shaving. *Applied Energy*, 147:246–257, 2015.